Accepted Manuscript

Title: Recent progress on the sensitive detection of cardiovascular disease markers by electrochemical-based biosensors

Authors: Nurgul K. Bakirhan, Goksu Ozcelikay, Sibel A. Ozkan

PII: S0731-7085(18)30806-9
DOI: https://doi.org/10.1016/j.jpba.2018.07.021
Reference: PBA 12092

To appear in: *Journal of Pharmaceutical and Biomedical Analysis*

Received date: 26-4-2018
Revised date: 7-7-2018
Accepted date: 16-7-2018

Please cite this article as: Bakirhan NK, Ozcelikay G, Ozkan SA, Recent progress on the sensitive detection of cardiovascular disease markers by electrochemical-based biosensors, *Journal of Pharmaceutical and Biomedical Analysis* (2018), https://doi.org/10.1016/j.jpba.2018.07.021

This is a PDF file of an unedited manuscript that has been accepted for publication. As a service to our customers we are providing this early version of the manuscript. The manuscript will undergo copyediting, typesetting, and review of the resulting proof before it is published in its final form. Please note that during the production process errors may be discovered which could affect the content, and all legal disclaimers that apply to the journal pertain.

ACCEPTED MANUSCRIPT

Recent progress on the sensitive detection of cardiovascular disease markers by electrochemical-based biosensors

Nurgul K. Bakirhan [1], Goksu Ozcelikay [2], Sibel A. Ozkan[2]*

[1]Hitit University, Faculty of Arts and Sciences, Department of Chemistry, Corum, Turkey

[2]Ankara University, Faculty of Pharmacy, Department of Analytical Chemistry, Tandogan, Ankara, Turkey

Corresponding author: ozkan@pharmacy.ankara.edu.tr

Highlights

- Cardiovasculer disease biomarkers were defined.
- Electrochemical studies of cardiovasculer disease biomarkers were presented according to the recent literture survey.
- Electrochemical cardiac sensors and fabrication materials were given in details.

Abstract

Cardiovascular disease is the most reason for deaths in all over the world. Hence, biomarkers of cardiovascular diseases are very crucial for diagnosis and management process. Biomarker detection demand is opened the important way in biosensor development field. Rapid, cheap, portable, precise, selective and sensitive biomarker sensing devices are needed at this point to detect and predict disease. A cardiac biomarker can be orderable as C-reactive protein, troponin I or T, myoglobin, tumor necrosis factor alpha, interleukin-6, interleukin-1, lipoprotein-associated phospholipase, low-density lipoprotein and myeloperoxidase. They are used for prediction of cardiovascular diseases. There are many methods for early diagnosis of cardiovascular diseases, but these have long time process and expensive devices. In recent studies, different biosensors have been developed to remove the problems in this field. Electrochemical devices and developed biosensors have many superiorities than others such as low cost, mobile, reliable, repeatable, need a little amount of solution. In this review, recent

ACCEPTED MANUSCRIPT

studies were presented as details for cardiovascular disease biomarkers detection using electrochemical methods.

Abbreviations:

$[Fe(CN)_6]^{3-/4-}$	:Potassiumferricyanide/ferrocyanide
4-ATP	:4-aminothiophenol
AChE	:Acetylcholine esterase
AdSSWV	:Adsorptive Stripping Square-wave voltammetry
Affibodys	:Combinatorial non-immunoglobulin protein
AG	:anodized graphene
Ag	:Silver
AgNp	:Silver Nanoparticle
Ag@Pt-CNTs–CS	:Bimetallic Ag@Pt core–shell nanoparticles functionalized carbon nanotube and chitosan
ALP	:Alkaline phosphatase
Anti-CRP	:Anti-C reactive protein antibody
Anti-cTnT(cTnI)	:Anti-cTnT(cTnI) monoclonal antibodies
Anti-MYO	:Anti-myoglobin antibody
Anti-TNF-α	:Anti-TNF- α antibody
Apt-Ag@Pt-GRs	:Bimetallic Ag@Pt core-shell nanoparticles functionalized graphene nanosheets
APTES	:3-aminopropyltriethoxysilane
ASV	:Anodic stripping voltammetry
Au	:Gold
Au(MPA)	:3-mercaptopropionic acid functionalized gold nanoparticles
AuNp	:Gold Nanoparticles
BP	:Monolayer black phosphorus
C60–CNTs–IL	:Fullerene functionalized carbon nanotubes and ionic liquid
CB	:Cucurbituril 7
CILE	:Carbon ionic liquid electrode
CK-MB	:Creatine kinase isoenzyme
CMA	:4-carboxymethyl aryl diazonium
CNF	:Carbon nanofiber
CNT	:Carbon nanotubes
COOH-GR	:Carboxylated graphene
COOH-PVC	:Carboxylated poly(vinyl chloride)
COOH–CNT	:Carboxylated carbon nanotubes
CS	:Chitosan
CTS- AuNPs	:Chitosan-stabilized gold nanoparticles
CV	:Cyclic voltammetry
DApt	:Y-shape structure of dual-aptamer
Den	:Dendrimer
DOXh	:Doxorubicin hydrochloride
DPV	:Differential pulse voltammetry

ACCEPTED MANUSCRIPT

DSP	:Dithiobis-succinimidyl propionate
STV-DSP	:Streptavidin-functionalized with dithiobis (succinimidyl propionate)
EA	:Ethanol amine
EDOTPC	:Poly(3,4-ethylenedioxythiophene (EDOT))- zwitterionic PC
EIS	:Electrochemical impedance spectroscopy
Exo I	:Exonuclease I
Fc	:Ferrocene
Fc-PNW	:Ferrocene functionalized peptide nanowire
FME	:Fiber microelectrode
FNAB	:4-fluoro-3-nitro-azidobenzene
FTO	:Fluorine doped tin oxide
GA	:Gluteraldehyde
GCE	:Glassy carbon electrode
GCF	:Gingival crevicular fluid
GMI	:Giant magnetoimpedance
GNR	:Gold nanorod
GQD	:Graphene quantum dots
GS	:Graphene nanoplatelets
HEP	:Heparin
HEPES buffer	:4-(2-hydroxy-ethyl)-1-piperazineethanesulfonic acid
HOOC-Phe-DWCNTs	:4-carboxyphenyl-functionalized double-walled carbon nanotubes
IDA	: interdigitated array
IgG	:Immunoglobulin
ITO	:Indium tin oxide
K-CS-GA	:$K_3[Fe(CN)_6]$-chitosan-glutaraldehyde
MBA	:Mb-binding-aptamer
MBs	:Magnetic beads
MEEPS	:Miniaturized electrophoresis electrochemical protein sensor
MES	:2-(N-morpholino)ethanesulfonic acid
MHA	:6-mercaptohexanoic acid
Mn_3O_4-RGO	:Manganese-reduced graphene oxide
Mo	:Molybdenum
MoS_2–PANI–GNP	:Molybdenum disulfide–polyaniline–gold nanoparticles
MPO	:Myeloperoxidase
MUA	:Mercaptoundecanoic acid
MWCNT	:Multiwalled carbon nanotubes
MYO	:Myoglobin
NCD	:Aldehyde-terminated nanocrystalline diamond
NEA	:Nanoelectrode arrays
NH_2-CNT	:Amine-functionalized carbon nanotubes
NHS	:N-Hydroxy succinamide
NT-proBNP	:Amino- terminal pro-B-type natriuretic peptide
p-NPP	:Para-Nitrophenylphosphate
P3	:Poly(3-thiophene acetic acid)
PAMAM	:Polyamidoamine

ACCEPTED MANUSCRIPT

PANI	:Polyaniline
PAP	:Poly(o-aminophenol)
PPAP	:p-aminophenyl phosphate
PB-CeO_2	:Prussian Blue (PB) functionalized ceria nanoparticles
PBS	:Phosphate buffered solution
PC	:Porous polycarbonate
Pcrea	:Phosphorylated form of creatine
PDDA	:Poly(diallyldimethylammonium chloride)
PDMS-GNP	:Poly(dimethylsiloxane)-gold nanoparticles
PEC	:Photoelectrochemical immunoassay
PEI	:Polyethyleneimine
PHE	:Amino acid phenylalanine
PLL	:Poly-L-lysine
PNW	:peptide nanowire
PPy	:Polypyrrole
PPy-PPa	:Poly(pyrrole- co-pyrrolepropylic acid)
Pt(MPA):	:3-Mercaptopropionic acid functionalized Platinium nanoparticles
PyNHS:	:1-pyrenebutyric acid N-hydroxy succinimide ester
PQI	:p-quinoneimine
rGO	:Reduced graphene oxide
SAM	:Self-assembled monolayer
SB	:Block T20
sCD40L	:Soluble CD40 ligand
SPAM	:Smart plastic antibody material
SPE	:Screen printed electrode
STV-PbS QDs	:Streptavidin-conjugated PbS quantum dots
SWV	:Square wave voltammetry
TCPP–Gr	:Meso-tetra (4-carboxyphenyl) porphyrin-functionalized graphene
TEPA	:Tetraethylene pentamine
Ti-NT	:Hydrothermally synthesized TiO_2 nanotubes
TMB	:3, 3′,5, 5′-tetramethyl benzidine
VACNFs	:vertically aligned carbon nanofibers
xGnP	:Exfoliated graphite nanoplatelets
ZnS(MPA)	:3-Mercaptopropionic acid functionalized ZnS nanocrystals

Keywords: Cardiovascular disease; biomarker; electrochemical-based biosensors

INDEX

ACCEPTED MANUSCRIPT

ACCEPTED MANUSCRIPT

1. Introduction

Cardiovascular diseases (CVD) is recognized as disorders of the heart and blood vessels and include coronary heart disease, cerebrovascular disease, rheumatic heart disease and other conditions. According to World Health Organization (WHO), a forecasted approximately 20 million (31%) of all global deaths in 2015 are related to CVD in both developed and developing countries [1]. The most common causes of cardiovascular disease are unhealthy nutrition, obesity, tobacco, use, alcohol use, stress and physical inactivity [2]. Trends in improvements in overall cardiovascular health metrics are projected to reduce cardiovascular disease deaths by 30% between 2010 and 2020 [3].

HERE FIGURE 1

The early detection and management of cardiovascular disease play an important role in clinical diagnosis for people with cardiovascular disease or who are at high cardiovascular risk. It is notable that not for only providing timely, life-saving therapeutic intervention but also reduce the costs for healthcare. The CVD is the key risk to human health. There is a growing demand because of many reasons. Therefore, mobile, miniaturization, accurate, rapid, sensitive and reliable, affordable sensing devices are developed for the detection of CVD [4]. Nowadays, it is well known that biomarkers which are identified CVD bridge over determining specific blood

ACCEPTED MANUSCRIPT

compounds (biomarkers) or variation of their concentrations identify various diseases in terms of CVD [5].

Biomarkers are one such tool that might improve identification of high-risk patients for CVD events and help guide treatment [6]. There are various type of biomarkers within the blood serum or plasma such as C-reactive protein (CRP), creatine kinase-MB (CK-MB), creatine kinase MM (CK-MM), myoglobin (MYO), interleukins (IL-1β, IL-6,IL-8), cardiac troponins (cTnI & cTnT), tumour necrosis factor alpha (TNF-α), NT-proBNP, Heart-type fatty-acid-binding protein (H-FABP) and etc. [6–8].

Identification of specific protein biomarkers for an early diagnosis and effective treatment of stroke and other cardiovascular disease risk and inflammation has been tested by various techniques [9]. Classical techniques of diagnosis for CVDs count on classical methods with difficulty such as surface plasmon resonance (SPR), immunoassays, enzyme-linked immunosorbent assay (ELISA) and Liquid Chromatography (LC) which are based on tests administered in central laboratories that may have long procedure when tests are from ordered to received [4].

Biosensors are also classified with regard to the selection rules of the analyte of interest: immunosensors which are antibody-antigen interaction and enzyme–target analyte interaction which is called as enzymatic biosensors and also nucleic acid based biosensors. All classical (enzymes, antibodies and DNA) and recent recognition elements play an important role in chemical sensors and biosensors using identify the target analytes of interest [10]. The electrochemical immunosensors rely on the measurements of currents and/or voltage to detect binding between antibody and antigen [11-13]. These sensors have some advantages such as cheapness, sensitivity, portability, disposability, the possibility of simultaneous multi analysis, reliability, small amounts samples and fast response. Hence, immunosensors have great interest by researchers. The regeneration of the binding sites on antibody may be problem. This procedure takes time and can damage to the binding sites. Therefore, lifetime of the antibodies may decrease. DNA biosensors offers sensitive and fast sequence-specific information [14]. Unlike enzymes or antibodies, DNA based biosensors can be readily synthesized and regenerated for multiple uses. Molecular diagnostics, pharmacogenomics, medical diagnosis, food analysis, environmental monitoring, bioterrorism, drug screening may be studied with DNA biosensors. The disadvantages of this sensor are ordered as the ability to perform direct signal transduction avoiding the images processing and statistical analysis and need automation of the detection step [15].

ACCEPTED MANUSCRIPT

Many researchers have studied methods for each developed biosensors which are electrochemical (amperometry, potentiometry, conductometry), optical (fluorescence, luminescence, refractive index), field-effect transistor, capacitor-based biosensors, piezoelectric or calorimetric for the detection of different biomarkers [11, 16, 17]. Electrochemical biosensors may be considered as an alternative to classical analysis for cardiac biomarkers. It presents many advantages such as user-friendly, rapid, robust, low-cost and capable of multianalyte testing [18]. Biosensor developing procedure does not need expensive and time-consuming laboratory tests. Thus, the cost of healthcare services is minimized.

In recent years, nanomaterials are used in biosensors. Nanomaterials have many properties for their conductive properties, high surface/volume, and good biocompatibility by this way enhancing performance [19–21]. To detection of clinically significant biomarkers, the following nanomaterials have been incorporated into biosensors: carbon-based nanomaterials (graphene, carbon nanotubes (CNT), metal nanoparticles (Ag, Au, Pt, Cu), semiconductors quantum dots (Cd, Se, Ge, Te), metal oxides (ZnO, CeO_2 and Al_2O_3) and silicon/ indium/gallium etc. [10, 22–24]. Gold based structures (screen printed electrode (SPE) or nanomaterials) are considered as a significant building to be used for the construction of (bio/nano) sensing because of their excellent mechanical, electrical and optical properties [25].

In this review; cardiovascular disease biomarkers, the importance of biosensor fabrication, the most used nanomaterials in biosensors, electrochemical methods and the literature survey of last decade on CVD biomarkers detection via electrochemical methods will be presented.

2. CVDs Markers

2.1.1 Cardiac Troponin

Cardiac troponin has a great specific biomarker compared to other biomarkers of myocardial injury. These are can be ordered as CRP, Interleukin, αTNF, CK-MB isoenzyme, MYO, Troponin which is classified as a complex of three regulatory troponin C, cTnI, and cTnT proteins. These are biomarkers for clarifying acute myocardial infarction (AMI) diagnosis [26].

cTnT is widely used as a specific biomarker for myocardial tissue and it is considered as “gold standard” because of producing solely in the myocardium and having a specific indication for cardiac injury. cTnT is suddenly released into the blood circulation. Therefore, the rapid and accurate monitoring of these biomarkers should be improved to increase the quality of patient

ACCEPTED MANUSCRIPT

life [27]. Biosensor could be developed for the accurate diagnosis of the cTnI biomarker since measurements made with an electrocardiogram usually produce erroneous and slow results [28]. Li and co-workers improved a novel immunosensor using immobilized antibodies on the graphene modified SPE for cTnT detection. The use of graphene material for electrode modification has the importance owing to the electrochemical activity of graphene. In this result, graphene considerably increased the sensitivity of cTnT showing a curve with a linear response range of 0.01 ng mL^{-1} to 1 ng mL^{-1} of cTnT and a limit of detection (LOD) of 0.005 ng mL^{-1}. It was also performed for the determination of cTnT in human serum samples. This immunosensor have promise for Point of Care (POC) quantitative testing of cTnT [29]. Ahammad et al. reported clinical applications of cTnI immunosensor, based horseradish peroxidase (HRP)-labeled probe. In this report, amperometry was used to detect cTNI with functionalized platinum nanoparticles (PtNPs) immobilized on a graphene (GR) monolayer modified glassy carbon electrode (GCE), obtaining detection between 1 and 100 ng mL^{-1} [30]. Biocompatible and flexible immunosensor based on the ionic organic molecule and chitosan-stabilized gold nanoparticles (ionic organic molecule/ CTS- AuNPs) was developed to detect TNF-α by Electrochemical Impedance Spectroscopy (EIS) [31]. Silva and coworkers were developed an immunosensor for cTnT detection. Streptavidin polystyrene microspheres on SPE fabricated as a biosensor to increase the electrochemical answer of cTnT. SEM and CV methods were used for the surface characterization of the biosensor (Figure 2). The modified electrode increased response of cTnT about 8.5 times of bare SPE. The linearity response was obtained between 0.1 and 10 ng mL^{-1}. 0.2 ng mL^{-1} was obtained as detection limit value [32].

HERE FIGURE 2

Recent studies on cardiac troponin biomarkers detection by electrochemical methods are presented in Table 1.

HERE TABLE 1

2.1.2. C-Reactive Protein

CRP is presented as a significant biomarker for the early detection of cardiovascular events and to prevent increasing the death rate because of the AMI [56]. CRP is a pentraxin protein (namely acute phase protein) which is produced by the liver [57–59]. It has been identified as a

ACCEPTED MANUSCRIPT

biomarker for atherosclerosis and inflammatory processes, since the concentration of these biomarker increases in the plasma of patients with such processes [60]. It is generally accepted as a component of plasma; concentration in plasma is less than 2.0 mg L^{-1} for healthy individuals and in the acute phase of inflammation, the concentration increases to 1,000 fold [61]. According to American Heart Association and the United States Centers for Disease Control, there are three different levels of CRP concentrations in human blood serum:

Concentration of CRP <1 mg mL^{-1} → a low-risk state,

1< concentration of CRP <3 mg mL^{-1} → average risk

Concentration of CRP >3 mg mL^{-1} → high risk

The reliable and early quantification of this target is often then cited to improve the outcome of cardiovascular or inflammatory disease [56]. Centi et.al. presented an electrochemical CRP aptasensor with monoclonal antibody and alkaline phosphatase as enzymatic label [62]. Kokkinos et.al. investigated electrochemical analysis of CRP using a SPE modified QDs [63]. Gupta and coworkers developed a label-free electrochemical biosensor for CRP using carbon nanofiber [56]. Mishra et al. investigated the electrical and sensing properties of ZnS (MPA)-PPy composite film for a-CRP in aqueous solution with impedance measurements [64]. Yagati and coworkers were developed label-free and direct detection of CRP via reduced graphene oxide nanoparticles modified ITO electrode (rGO-NP-ITO). The response was applied by EIS with 1 ng mL^{-1} and 1000 ng mL^{-1} linearity range (Figure 3) [65].

HERE FIGURE 3

It is developed a potentiometric biosensor based on the antibody immobilized ZnO nanotubes achieving detecting linear range 10^{-5} mg L^{-1} and 1.0 × 100 mg L^{-1} within buffer medium [66]. Other recent studies for CRP biomarker detection are shown in Table 2.

HERE TABLE 2

2.1.3. Tumor necrosis factor alpha (TNF-α)

ACCEPTED MANUSCRIPT

One of the specific cardiac biomarkers is TNF- α, which is synthesized by immunological and non-immunocellular cells [96, 97]. In last years, there are intensive studies to develop new technologies for TNF-α Diagnosis and detection [98]. EIS was applied to measure TNF-α using anti-TNF-α-immobilized over CMA-modified gold microelectrodes, achieving detection between 266 pg mL^{-1} and 666 ng mL^{-1} [99]. Similarly, a sensitive and disposable immunosensor based on SB/EA/anti-TNF-α/DTSP/Au electrodes was used to measure TNF-α by EIS. Immunosensors were applied for whole serum with high sensitivity [100]. It is developed a novel and sensitive label-free electrochemical immunosensor based on entrapping of an anti-TNF-α onto nanocomposite including fullerene-functionalized multiwalled carbon nanotubes and an ionic liquid. LOD for TNF-α is 2.0 pg mL^{-1}. A novel immunosensor is applied to the human serum [101]. In another relevant study, Kongsuphol and coworkers presented gold microelectrodes array to considerably increase the sensitivity of TNF-α. This immunosensor has reached the success with a limit of detection (LOD) of 1 pg mL^{-1} [102]. Sànchez-Tirado et al. show that the dual cardiac biomarkers (IL-1b and TNF- α) could be detected and quantified using sensitive and notable immunosensor. The simultaneous dual immunosensor allows linearity obtaining between 0.5 and 100 pg mL^{-1} and from 1 to 200 pg mL^{-1} for IL-1b and TNF-a, respectively [103]. Li and coworkers detected TNF- α using Prussian blue functionalized ceria nanoparticles (PB-CeO_2) as a label. The sandwich type biosensor was designed via immobilization of anti-TNF-α on gold nanoparticles modified carbon nanotube surface. The answer of the biosensor was checked by peroxide signal between 0.005–5 ng mL^{-1} with 2 pg mL^{-1} detection limit (Figure 4) [104]. The other published studies on TNF-α biomarkers are presented in Table 3.

Commented [EZ1]: WC – this doesn't make sense

HERE FIGURE 4

HERE TABLE 3

2.1.4. Myoglobin

MYO is a non-enzymatic cardiac protein, originates in the blood and skeletal muscle in response to damage to the heart, and is being extensively used as a diagnostic marker of AMI. During AMI, the small-sized MYO (17.8 kDa) releases within 1-3 h in blood circulation and its level rises to as high as 900 ng mL^{-1} from its normal value of 30 to 90 ng mL^{-1}. The high

ACCEPTED MANUSCRIPT

sensitivity and high predictive value of MYO make it an important screening test for AMI [128]. MYO is one of the earliest biomarkers of acute myocardial infarction. Its express determination in blood is very important in clinical diagnostics [129]. MYO is present in very low concentrations (below 0.01 μg mL^{-1}) in the urine of healthy individuals. In a severe muscle damage, the concentration of MYO appears at extremely high levels (750 μg mL^{-1}). The MYO level in the serum is detected to be 0.008 to 0.098 μg mL^{-1} for healthy individuals and in a condition where there is muscle damaged, the concentration of MYO increases to 79.9 μg mL^{-1} [130]. Szymanski et al. show that, by using this novel electrochemical sandwich immunoassay, the cardiac biomarker could be detected and quantified. LOD for MYO is 3.0 ng mL^{-1} [131]. It is developed an electrochemical impedance MYO immunosensor based on bio-recognition element immobilization on the surface of the transducer achieving detection between 350 ng mL^{-1} to 17.5 μg mL^{-1} within phosphate buffered saline or the whole serum [132]. Ribeiro and co-workers fabricated an MYO biosensor with MIP polyphenol modified AuSPE. Polymer thickness was studied and found as about 4.4 nm. The linearity range was obtained between 0.001 ng mL^{-1} to 100 μg mL^{-1} (Figure 5) [133]. Tyrosine kinase AXL is a receptor, which is known as an inflammatory biomarker in acute coronary syndrome [134]. It's cut-off level value is 71 ng mL^{-1} [135]. Serafin and coworkers designed an amperometric disposable immunosensor for receptor tyrosine kinase AXL using poly(pyrrolepropionic acid)-modified SPE. This biosensor gave 337 pg mL^{-1} as LOD with a good selectivity in serum sample. The results were obtained with a excellent agreement with ELISA [136]. Recent studies with electrochemical methods for MYO detection are given in Table 4.

HERE FIGURE 5

HERE TABLE 4

2.1.5. Biosensors for CVDs Markers

Sensors, especially biosensors are defined as analytical devices that have a biological sensor in their body and are combined with a physicochemical transducer. The purpose of a biosensor is to generate a continuous digital electrical signal proportional to the quantity of one or more analytes to be analyzed. Bioensors are generally constructed by combining a bioactive component that interacts selectively with the substance to be analyzed, with a conduction

ACCEPTED MANUSCRIPT

system that transmits the resulting signal. As biocomponents in biosensors, enzyme cultures, microorganisms, organelles, antibodies and nucleic acids can be used as amperometric, potentiometric, thermal, piezoelectric, acoustic or optical sensors. In addition to the high specificity of sensors, they have the advantage of allowing direct measurement in a wide range of concentrations in colored and turbid solutions. However, the influence of environmental conditions such as pH, temperature, and ionic strength can decrease the life of the biosensor.

Biosensors have developed for the detection of CVDs biomarker. Several nanomaterials have been used for these biosensors fabrication. Nanotubes, nanowires, metal nanoparticles and polymer-based modifications are mostly preferred in these studies due to their improving responses of analytes, increasing surface area, sensitivity, selectivity properties [76,165–167]. The increasing concentrations of cardiac biomarkers in serum are very important because of CVD events and high death rates. Hence, fast, reliable, precise detections of these biomarkers are very crucial. The significant concentration of CVD biomarkers is changed between pM to nM, so their assay methods also need to be highly sensitive. These biomarkers cut of levels in serum samples are given following Table 5 [168]:

HERE TABLE 5

2.2. Transducer Types for Detection of CVDs Biomarkers

The performance of the electrochemical method depends on the material of the transducers. The working electrode is a substrate in these experiments. It should be given a low noise signal and repeatable answers for analytes. Factors such as potential range, electrical conductivity, surface reproducibility, mechanical properties, cost and toxic effects also play an important role in the electrode selection. The most preferred electrodes are noble metal electrodes such as mercury, carbon-based, platinum and gold. Especially, solid electrodes are preferred due to the disadvantages of the mercury electrodes. It has a narrow potential range in anodic part so that oxidation of compounds or biological molecules cannot be studied. Platinum, gold, silver and other noble metals and carbon-based materials, as well as nickel and copper electrodes, are used as a substrate. Gold and platinum electrodes have a wide range of potential and they have also fast electron transfer mechanism. A gold electrode is more inert than platinum. Glassy carbon

ACCEPTED MANUSCRIPT

and new trend screen printed electrodes (SPE) are also referred as carbon-based transducers [18, 42, 46, 47, 61-63, 66-68, 71, 113, 127]. Gold screen-printed electrodes (Au-SPE) have been studied in several studies for detection of CVDs biomarkers [70,117]. Modified electrodes are most preferred substrates for detections. The new electrode surface can be designed with different modification steps. The modification process is achieved selectivity and sensitivity features to the substrate. Modifiers should be conductive. These electrodes have several superiorities, as follows:

- The chemical substances that can be used in the modification process are unlimited.
- The electrode surface is covered with various molecules, can be reduced or increased accordingly.
- Surfaces with high sensitivity to certain types can be formed.
- More durable surfaces can be obtained for corrosion and other factors.
- Surface modification and electron transfer mechanism can be explained.

Carbon is a conductive modifier that has many types such as single crystal graphite, pyrolytic graphite, powdered graphite, carbon black and glassy carbon. The desired modifications are prepared by various methods such as reduction with diazonium salts, oxidation with alcohol and amines, self-assembled layers, Langmuir-Blodgett surfaces, carbon nanotubes, metal nanoparticles and quantum dots, chemical modification processes, plasma, and ion bomber ways.

2.3. Nanomaterials on Transducer Design for Cardiovascular Disease Markers Detections

In last years, the sensitivity analysis of biomolecules is of prime importance in the area of medical diagnostics. CVDs are cited as one of the most serious threats to global health [169]. Hence, the sensitivity analysis of cardiac biomarkers plays an important role in diagnosis and screening of CVDs. Nanomaterials have common usage in the detection of biomolecules as sensitively. People have a great interest in these materials due to their nano functionality, biological properties, and unique physical and chemical characteristics. They can be in the prism, rod, cube, ball and needle forms with 5-100 nm size colloids. Metal-based nanomaterials have a new area of interest in all branches of science related to their outstanding features [170]. They have well antimicrobial features because of their large surface area to volume ratio. Hence, they can be used in different biosensor development studies and as effective growth inhibitors of various microorganisms. Furthermore, nanomaterials can be modified to achieve

ACCEPTED MANUSCRIPT

better efficiency and to facilitate their applications in different fields such as biomaterials and medicine. Nanotechnology is making today's products smaller, stronger, lighter, faster and more durable.

Carbon nanomaterials have excellent features such as a high electrical conductivity, high surface-to-volume ratio, biocompatibility, robust mechanical strength, chemical stability [171,172]. Hence, these features, they can be preferred as sensing compounds. Carbon based biosensors have high sensitivity so that they can sense very low detections of analytes [173]. The surface characteristics of carbon-based nanomaterials include a critical factor that enables their functionality and stable operation in the design of efficient electrochemical biosensors; all of which impart effects on their electron transport kinetics [174].

For instance, in vivo, and in vitro studies can be performed with carbon nanotubes as carbon-based nanomaterials. Carbon nanotubes modified biosensors may achieve very sensitive detection of biomolecules [175]. Also, carbon nanohorns and nanofibers are new materials in science that they have been reported as novel and biocompatible matrices for many biological studies [176]. Graphene is the other carbon-based material that used in the very wide area due to their unique physical and chemical properties of two-dimensional material [177]. Nanotechnology has great interest in it in recent years. Babak Rezaei et.al. detected cTnI at a sandwich-type nanostructured immunosensor based on carboxylated multi-walled carbon nanotube (CMWCNT)-embedded whiskered nanofibres (WNFs) modified glassy carbon electrode (Figure 6). The amperometric method was applied and linear ranges were obtained between for a normal person 0.5 and 2 ng mL^{-1} to the concentration present in myocardial infarction patients (> 20 ng mL^{-1}), with a detection limit of 0.04 ng mL^{-1}. The developed substrate had repeatability and reproducibility [178]. Hence, the proposed biosensor presented the potential for point-of-care testing.

HERE FIGURE 6

To selective and sensitive determination of cTnI was studied by Fereshteh Chekin and coworkers at nitrogen-doped reduced graphene oxide (N-prGO) modified glassy carbon electrode. A label-free electrochemical biosensor showed good sensitivity with 1 pg mL^{-1} in human serum via differential pulse voltammetry. The successful detection could be obtained by site-specific surface modification [179]. Surface characterization was studied with CV, XPS and SEM (Figure 7).

ACCEPTED MANUSCRIPT

HERE FIGURE 7

Noble metal nanoparticles have common usage in sensing technology with unique optoelectronic (size and shape), magnetic and chemical properties. Platinum, gold and silver are the most widely studied particles for sensitive biomolecule detection, molecular diagnostic, drug delivery, imaging and therapeutics [180]. These metals have easily characterization, short synthesis process and enable to surface functionalization properties.

Platinum nanoparticles especially have been selected for biomedical applications due to their optoelectronics features. Nanoparticles that used in biological studies take superiority such as functional and dimensional characteristics of surfaces and inorganic cores that translates to specific physical properties.

HERE FIGURE 8

Patil and others were detected simultaneously Brain Natriuretic Peptide (BNP) and cTnT biomarkers by electrochemical impedance spectroscopy method. Various platinum wires were used for detection more sensitive and selective detection of these biomarkers. Different diameters of wires and surface preparation processes were tried at this point (Figure 8). Platinum wire with 0.5 mm diameter was found as best and it was polished to 5 μm that showed linearity, precision, and sensitivity for detecting Brain Natriuretic Peptide and cTnT [181].

Gold nanoparticles as a type of noble metal materials have many studies in the electrochemical field. Gold nanoparticles have excellent stability, good biocompatibility, easy synthesis process, large surface area to volume ratio. They are also used as a catalyst in many biomedical studies. Nanotechnology is like smaller devices for sensing, gold nanoparticles are redox active particle so that they can be used for miniaturization of devices. Gold based nanoparticles have application in both macro and nanoscale science. They can be used in medicine as the treatment of diseases. They make a tremendous impact in the biomedical area due to their less hazardous and non-interference with other labeled biomaterials (e.g., antibody and other biomarkers) [182].

HERE FIGURE 9

ACCEPTED MANUSCRIPT

Zapp and coworkers were detected MYO on the ionic liquid crystal (E)-1-decyl-4-[(4-decyloxyphenyl)diazenyl]pyridinium bromide (Br–Py) coated on a glassy carbon electrode (Figure 9). The monoclonal anti-myoglobin antibody (anti-MYO) was covalently immobilized by glyoxal on a film of polyethyleneimine-coated gold nanoparticles (AuNp-PEI). The developed biosensor performance was tested by electrochemical impedance spectroscopy method with 9.96–72.8 ng mL^{-1} linear range and 6.29 ng mL^{-1} detection limit of MYO biomarker [183].

Silver nanoparticles are also important substances in nanoscience and biosensing technology but it has not been studied as gold nanoparticles. Silver nanoparticles based specific and sensitive biosensors have the possible opportunity like creating new diagnostic platforms for biological and infectious agents, disease markers in the early-stage detection of disease and other physiological threats [184,185]. Guifen Jie et al. demonstrated a biosensor that based silver nanoclusters for thrombin detection by DNAzyme-assisted target recycling and hybridization chain reaction multiple amplification strategy (Figure 10). DPV responses shows a linearity in 1.0 fM to 10.0 nM with a detection limit 0.1 fM [186].

HERE FIGURE 10

In the recent years, there has been great interest in polymers that have been used for biomolecule sensing. The preparation of synthetic molecular networks with designed artificial precognitive domains exhibiting tailored recognition and release features is beginning to attract the interest of the drug delivery scientists [187]. Imprinting technology applications are getting increasing numbers. They can be used in controlled-release carriers for therapeutic agents and diagnostic devices due to their applicability for a wide range of analytes, long stability and cheap preparation [188,189]. Molecularly imprinted polymers (MIPs) were conceived as artificial tailor-made receptors for molecular recognition. They have the chemical strength and robust mechanical characteristics of its cross-linked materials with selectivity and sensitivity for the target analyte that mimics of the natural receptors.

Kumar et al. studied with a CRP-imprinted polymer film onto the surface of screen-printed carbon electrodes for detection of CRP (Figure 11). The limit of detection was calculated as 0.04 μg mL^{-1}. 2-Acryl aminoethyl dihydrogen phosphate monomer was used with

ACCEPTED MANUSCRIPT

phosphatidylcholine as a natural binder. Molecularly imprinted polymer modified screen-printed electrode surface morphology characterization was applied with atomic force microscopy and scanning electron microscopy analyses [190].

HERE FIGURE 11

2.4. Electrochemical Methods for Cardiovascular Disease Markers Detections

Early diagnosis of cardiovascular diseases has consequently become highly important to decrease mortality. To sensitive detection of cardiac biomarkers, several methods have been used in the literature such as fluorescence and chemiluminescence techniques [191] radioimmunoassay [192] ELISA [193]. However, these methods have many problems like long time and complicated processes; need a specialist for usage [194, 195]. Hence, the requirement of a more sensitive and easy method has been increased for the detection of cardiac biomarkers. At that point, electrochemical methods provide many advantages such as sensitive, selective, rapid, portability, low price, and simplicity. These methods can be applicable to many analytical chemistry fields. Especially, voltammetric techniques have a common use for the detection of biological substances, metabolites, and drugs.

Cyclic voltammetry (CV) and linear sweep voltammetry (LSV) have excellent techniques for the investigation of mechanisms. In the cyclic voltammetry technique, the scan speed is changed and the results of peak heights can be evaluated. From the rate of change in scan rate and peak heights, adsorption, diffusion, and electron transfer the presence or absence of chemical reaction events and their size can be determined.

Bhatnagar et al. used CV method for detection of cTnI antibody conjugated with graphene quantum dots and polyamidoamine nanohybrid modified gold electrode. 4-Aminothiophenol was used for amine functionalization of the screen printed gold electrode surface. The amino groups were coupled with carboxyl functionalities of GQD with EDC-NHS reaction. PAMAM dendrimer was embedded on GQD through carbodiimide coupling to provide an ultra-high surface area for antibody immobilization. The linearity range was obtained by cyclic voltammetry between 10^{-6} and10 ng per 6 µL cTnI in serum and the limit of detection was found 25 fg mL^{-1} [33].

ACCEPTED MANUSCRIPT

For the sensitive detection of compounds, differential pulse voltammetry (DPV) and square wave voltammetry (SWV) have been used. Centi et al. studied on sensitive detection of CRP in serum. The assay was based on a sandwich format in which an RNA aptamer was coupled to a monoclonal antibody and alkaline phosphatase (AP) was used as an enzymatic label. Enzymatic reaction results were investigated by DPV method. All DPV method parameters were optimized to obtain high sensitivity and specificity. CRP could be successfully detected at the optimized conditions in serum samples [62].

Sun and coworkers studied on sensitive detection of tumor necrosis factor α. This biomarker based on dual signal amplification of ferrocene modified self-assembled peptide nanowire and glucose oxidase functionalized gold nanorods were developed. Ferrocene carboxylic acid functionalized self-assembled peptide nanowire could increase the surface area. Ferrocene carboxylic acid can catalyze the glucose reaction. Gold nanorods achieved high sensitivity for tumor necrosis factor α with a wide linear range between 0.005 and10 ng mL^{-1} [110].

A disposable electrochemical assay involving magnetic particles and carbon-based screen-printed electrodes (SPCEs) was developed for the detection of CRP. CRP is a plasma protein and is among the most expressed proteins in acute phase inflammation cases, being a known biomarker for inflammatory states. The assay was based on a sandwich format in which an RNA aptamer was coupled to a monoclonal antibody and alkaline phosphatase (AP) was used as an enzymatic label. After the sandwich assay, the modified magnetic beads were captured by a magnet on the surface of a graphite working electrode and the electrochemical detection was thus achieved through the addition of the AP substrate (a-naphthyl-phosphate) and a-naphthol produced during the enzymatic reaction was detected using differential pulse voltammetry (DPV). The parameters influencing the different steps of the assay were optimized in order to reach the best sensitivity and specificity. With the optimized conditions, the assay was applied to the analysis of CRP free serum and serum samples.

Stripping voltammetry methods appreciate the ultra-trace detections via preconcentration of analytes. Szymanski et al. developed a validated anodic stripping voltammetry method for detection of MYO. They used silver nanoparticles on a screen printed planar carbon electrode. They prepared a sandwich type immunosensor and could detect 3 ng mL^{-1} biomarker concentration [131].

The amperometric detection has common usage in electrochemical sensing analytes. In recent years, it has increased interest because of its high sensitivity, rapid and broad linear range. This method can be preferred for the development of portable smart immunosensors. Jo et al.,

ACCEPTED MANUSCRIPT

developed an amperometric method for the detection of cTnI. Disposable screen-printed carbon electrodes were used with various modifications such as gold nanoparticles and conducting polymers (Figure 12). The amperometric response was related to the catalytic reaction between hydrazine and hydrogen peroxide. The developed aptasensor was showed broad linear range between 0.024 and 2.4 ng mL^{-1} with a detection limit of 24 pg mL^{-1} that is lower than cut off levels of 40–700 pg mL^{-1} [196]. Electrochemiluminescent (ECL) and photoelectrochemical assays are also used for optical and electrochemical detection.

HERE FIGURE 12

EIS is also a very effective technique in biosensor studies. Impedance spectroscopy is an effective technique for investigating electrochemical systems and methods. All total resistance in a circuit is called impedance. EIS, unlike electrochemical techniques, both in volume studies and in interface operations that related with time constants. Furthermore, EIS is a method of electrochemical measurement of a wave signal at a small size, based on the perturbation of the cell. The applied potential for perturbation can be a wide range that the applied current or the velocity of convection in hydrodynamic electrodes [197]. Impedance depends on total change in the resistance which is affected by the capacitance and inductive changes. Whether or not the EIS data is correct is determined by an electrical circuit. This circuit involves three parameters such as resistor, capacitor, and inductor. The simplest cycle of the EIS is Randles circuit [198]. The solution resistor has a double layer capacitor and a charge transfer or polarization capacitor. EIS performs for label-free and rapid detection of ultra-low-concentration analytes. EIS can achieve rapid, label-free, and ultrasensitive biomarker detection and can measure multiple markers simultaneously [199–201].

Singal et al. developed a stable electrochemical impedance immunosensor with Pt nanoparticles with electrochemically oxidized graphene modified glassy carbon electrode to quantification of cTnI. 3-Mercaptopropionic acid (MPA) functionalized Pt-nanoparticles, Pt (MPA), were bound to electroactive graphene (EG) using 1-pyrenemethylamine (PMA). Carbodiimide coupling reaction was performed to form an anti-cTnI-Pt (MPA)-PMA/EG/GCE (Figure 13). This biosensor was detected cTnI in a wide linear range between 0.01 and 10 ng mL^{-1} in phosphate

ACCEPTED MANUSCRIPT

buffer saline (pH 7.4) with a sensitivity of 80 Ω cm^2 per decade and a limit of detection of 4.2 pg mL^{-1} cTnI [48].

HERE FIGURE 13

3. Conclusions and Future Perspectives

The cardiac biomarkers provide important information for clinicians by assisting in the guidance of diagnostic, prognostic, and treatment decisions for patients presenting urgently with signs and symptoms of myocardial infarction. According to the literature, published studies are increasing on detection of cardiac biomarkers. Several analysis and detection methods have been applied by optic, chemiluminescence, radioimmunoassay, enzyme-linked immunosorbent assay methods. These methods have several problems such as longtime consumption, expensive equipment, and pretreatment process. Unlike these mentioned methods, electrochemical methods have great features like rapid, mobile, cheap devices, reliable, precise and etc. In this review, it is aimed to present a summary of the recent studies on cardiovascular diseases biomarkers detections by electrochemical methods. According to the literature survey; SWV, DPV and EIS have been most preferred methods for detection of cardiac biomarkers. EIS method has been used generally for sensor morphology characterization to show different materials on sensor surfaces. SWV and DPV methods were optimized for sensitive detection of cardiovascular biomarkers.

The most used nanoparticles for fabrication of biomarker biosensors also are presented. According to the literature, gold and carbon based nanoparticles have very often usage for detection of cardiac biomarkers. Nanomaterials have great interest about their integration into biosensor devices since they can improve the detection sensitivity and limit of detection values. They are preffered due to their easy synthesis and easy integration to any type of sensors.

ACCEPTED MANUSCRIPT

Cardiovascular biomarker detection studies can be used in future at clinics due to their easy sample preparation for the measurements and fast application from blood or other biological samples from patients. Rapid and accurate diagnosis, risk stratification, and management decisions will continue to be aided by biomarkers. They play an invaluable role in providing effective care while minimizing healthcare costs. So that, many cardiovascular diseases can be predicted previously. In recent days, there has been growing interest to use lab-on a chip biosensors that is known as the mobile sensing based on smartphone and microfluidic devices. These devices have powerful imaging and computing capabilities to achieve fast data acquisition and reporting. These features are very important for personals and patients. In next future, lab-on a chip sensor will be used in cardiac diseases and other diagnosis of diseases.

ACCEPTED MANUSCRIPT

ACCEPTED MANUSCRIPT

References

[1] N.J Pagidipati, T.A. Gaziano, Estimating Deaths From Cardiovascular Disease: A Review of Global Methodologies of Mortality Measurement, Circulation, 127 (2013) 749–756. doi:10.1109/TMI.2012.2196707.

[2] Z. Altintas, W.M. Fakanya, I.E. Tothill, Cardiovascular disease detection using bio-sensing techniques, Talanta. 128 (2014) 177–186. doi:10.1016/j.talanta.2014.04.060.

[3] E.J. Benjamin, M.J. Blaha, S.E. Chiuve, M. Cushman, S.R. Das, R. Deo, S.D. De Ferranti, J. Floyd, M. Fornage, C. Gillespie, C.R. Isasi, M.C. Jim'nez, L.C. Jordan, S.E. Judd, D. Lackland, J.H. Lichtman, L. Lisabeth, S. Liu, C.T. Longenecker, R.H. MacKey, K. Matsushita, D. Mozaffarian, M.E. Mussolino, K. Nasir, R.W. Neumar, L. Palaniappan, D.K. Pandey, R.R. Thiagarajan, M.J. Reeves, M. Ritchey, C.J. Rodriguez, G.A. Roth, W.D. Rosamond, C. Sasson, A. Towfghi, C.W. Tsao, M.B. Turner, S.S. Virani, J.H. Voeks, J.Z. Willey, J.T. Wilkins, J.H.Y. Wu, H.M. Alger, S.S. Wong, P. Muntner, Heart Disease and Stroke Statistics'2017 Update: A Report from the American Heart Association, 2017. doi:10.1161/CIR.0000000000000485.

[4] A. Qureshi, Y. Gurbuz, J.H. Niazi, Biosensors for cardiac biomarkers detection: A review, Sensors Actuators, B Chem. 171–172 (2012) 62–76. doi:10.1016/j.snb.2012.05.077.

[5] B. Rezaei, M. Ghani, A.M. Shoushtari, M. Rabiee, Electrochemical biosensors based on nanofibres for cardiac biomarker detection: A comprehensive review, Biosens. Bioelectron. 78 (2016) 513–523. doi:10.1016/j.bios.2015.11.083.

[6] R.T. Dadu, V. Nambi, C.M. Ballantyne, Developing and assessing cardiovascular biomarkers, Transl. Res. 159 (2012) 265–276. doi:10.1016/j.trsl.2012.01.003.

[7] D.W. Kehl, N. Iqbal, A. Fard, B.A. Kipper, A. De La Parra Landa, A.S. Maisel, Biomarkers in acute myocardial injury, Transl. Res. 159 (2012) 252–264. doi:10.1016/j.trsl.2011.11.002.

[8] K. Thygesen, J.S. Alpert, H.D. White, Universal definition of myocardial infarction, Eur. Heart J. 28 (2007) 2525–2538. doi:10.1093/eurheartj/ehm355.

[9] S. Ray, P.J. Reddy, S. Choudhary, D. Raghu, S. Srivastava, Emerging nanoproteomics approaches for disease biomarker detection: A current perspective, J. Proteomics. 74 (2011) 2660–2681. doi:10.1016/j.jprot.2011.04.027.

[10] C.I.L. Justino, A.C. Duarte, T.A.P. Rocha-Santos, Critical overview on the application of sensors and biosensors for clinical analysis, TrAC - Trends Anal. Chem. 85 (2016) 36–60. doi:10.1016/j.trac.2016.04.004.

[11] S.A. Ozkan, Electroanalytical Methods in Pharmaceutical Analysis and Their Validation, (2012) 350. https://books.google.com/books?id=pIHjPQAACAAJ&pgis=1.

[12] A. Baraket, M. Lee, N. Zine, M. Sigaud, J. Bausells, A. Errachid, A fully integrated electrochemical biosensor platform fabrication process for cytokines detection, Biosens. Bioelectron. 93 (2017) 170–175. doi:10.1016/j.bios.2016.09.023.

[13] E. Burcu Bahadir, M. Kemal Sezgintürk, Applications of electrochemical immunosensors for early clinical diagnostics, Talanta. 132 (2015) 162–174. doi:10.1016/j.talanta.2014.08.063.

ACCEPTED MANUSCRIPT

[14] S. Hahn, S. Mergenthaler, B. Zimmermann, and W. Holzgreve: Nucleic acid based biosensors: The desires of the user. *Bioelectrochemistry* 67 (2005)151.

[15] F. Katagiri and J. Glazebrook: Overview of mRNA Expression Profiling Using DNA Microarrays. *Current Protocols in Molecular Biology* 85 (2009) 22.4.1

[16] Y. Cheng, K.-S. Chen, N. L. Meyer, J. Yuan, L. S. Hirst, P. B. Chase, and P. Xiong: Functionalized SnO2 nanobelt field-effect transistor sensors for label-free detection of cardiac troponin. *Biosensors and Bioelectronics* 26 (2011) 4538

[17] M. F. M. Fathil, M. K. Md Arshad, S. C. B. Gopinath, U. Hashim, R. Adzhri, R. M. Ayub, A. R. Ruslinda, M. Nuzaihan M N, A. H. Azman, M. Zaki, and T.-H. Tang: Diagnostics on acute myocardial infarction: Cardiac troponin biomarkers. *Biosensors & bioelectronics* 70 (2015) 209.

[18] B.E.F. de Ávila, V. Escamilla-Gómez, V. Lanzone, S. Campuzano, M. Pedrero, D. Compagnone, J.M. Pingarrón, Multiplexed determination of amino-terminal pro-B-type natriuretic peptide and C-reactive protein cardiac biomarkers in human serum at a disposable electrochemical magnetoimmunosensor, Electroanalysis. 26 (2014) 254–261. doi:10.1002/elan.201300479.

[19] C.I.L. Justino, T.A.P. Rocha-Santos, A.C. Duarte, Advances in point-of-care technologies with biosensors based on carbon nanotubes, TrAC - Trends Anal. Chem. 45 (2013) 24–36. doi:10.1016/j.trac.2012.12.012.

[20] C. Fenzl, T. Hirsch, A.J. Baeumner, Nanomaterials as versatile tools for signal amplification in (bio)analytical applications, TrAC - Trends Anal. Chem. 79 (2016) 306–316. doi:10.1016/j.trac.2015.10.018.

[21] M. Hasanzadeh, N. Shadjou, Electrochemical nanobiosensing in whole blood: Recent advances, TrAC - Trends Anal. Chem. 80 (2016) 167–176. doi:10.1016/j.trac.2015.07.018.

[22] N.J. Ronkainen, S.L. Okon, Nanomaterial-based electrochemical immunosensors for clinically significant biomarkers, Materials (Basel). 7 (2014) 4669–4709. doi:10.3390/ma7064669.

[23] C.I.L. Justino, T.A.P. Rocha-Santos, S. Cardoso, A.C. Duarte, S. Cardosa, Strategies for enhancing the analytical performance of nanomaterial-based sensors, TrAC - Trends Anal. Chem. 47 (2013) 27–36. doi:10.1016/j.trac.2013.02.004.

[24] M.J.A. Fernández-garcia, Rodriguez, Metal Oxide Nanoparticles, Nanomater. Inorg. Bioinorg. Perspect. (2007) 60. doi:10.1002/0470862106.ia377.

[25] A. Mozalev, H. Baccar, A. Abdelghani, Preparation and Biosensing Performance of Porous-alumina-Assisted Gold Nanostructures on Substrates, Procedia Eng. 168 (2016) 1188–1191. doi:10.1016/j.proeng.2016.11.404.

[26] M. Abdorahim, M. Rabiee, S.N. Alhosseini, M. Tahriri, S. Yazdanpanah, S.H. Alavi, L. Tayebi, Nanomaterials-based electrochemical immunosensors for cardiac troponin

ACCEPTED MANUSCRIPT

recognition: An illustrated review, TrAC - Trends Anal. Chem. 82 (2016) 337–347. doi:10.1016/j.trac.2016.06.015.

[27] D. Brondani, J.V. Piovesan, E. Westphal, H. Gallardo, R.A. Fireman Dutra, A. Spinelli, I.C. Vieira, A label-free electrochemical immunosensor based on an ionic organic molecule and chitosan-stabilized gold nanoparticles for the detection of cardiac troponin T, Analyst. 139 (2014) 5200–5208. doi:10.1039/C4AN00993B.

[28] X. Han, S. Li, Z. Peng, A.M. Othman, R. Leblanc, Recent Development of Cardiac Troponin I Detection, ACS Sensors. 1 (2016) 106–114. doi:10.1021/acssensors.5b00318.

[29] Z. Li, L. Geng, T. Feng, J. Wang, Electrochemical determination of cancer and cardiovascular biomarkers based on advanced screen-printed immunosensors, Int. J. Electrochem. Sci. 11 (2016) 9438–9446. doi:10.20964/2016.11.41.

[30] A.J. Saleh Ahammad, Y.H. Choi, K. Koh, J.H. Kim, J.J. Lee, M. Lee, Electrochemical detection of cardiac biomarker troponin I at gold nanoparticle-modified ITO electrode by using open circuit potential, Int. J. Electrochem. Sci. 6 (2011) 1906–1916.

[31] B.V.M. Silva, I.T. Cavalcanti, A.B. Mattos, P. Moura, M.D.P.T. Sotomayor, R.F. Dutra, Disposable immunosensor for human cardiac troponin T based on streptavidin-microsphere modified screen-printed electrode, Biosens. Bioelectron. 26 (2010) 1062–1067. doi:10.1016/j.bios.2010.08.051.

[32] B. V. M. Silva, I. T. Cavalcanti, A. B. Mattos, P. Moura, M. D. P. T. Sotomayor, and R. F. Dutra: Disposable immunosensor for human cardiac troponin T based on streptavidin-microsphere modified screen-printed electrode. *Biosensors and Bioelectronics* 26 (2010) 1062.

[33] R. Akter, B. Jeong, Y.M. Lee, J.S. Choi, M.A. Rahman, Femtomolar detection of cardiac troponin I using a novel label-free and reagent-free dendrimer enhanced impedimetric immunosensor, Biosens. Bioelectron. 91 (2017) 637–643. doi:10.1016/j.bios.2017.01.021.

[34] D. Bhatnagar, I. Kaur, A. Kumar, Ultrasensitive cardiac troponin I antibody based nanohybrid sensor for rapid detection of human heart attack, Int. J. Biol. Macromol. 95 (2017) 505–510. doi:10.1016/j.ijbiomac.2016.11.037.

[35] E. Dempsey, D. Rathod, Disposable Printed Lateral Flow Electrochemical Immunosensors for Human Cardiac Troponin T, IEEE Sens. J. 18 (2018) 1828–1834. doi:10.1109/JSEN.2018.2789436.

[36] S.L.R. Gomes-Filho, A.C.M.S. Dias, M.M.S. Silva, B.V.M. Silva, R.F. Dutra, A carbon nanotube-based electrochemical immunosensor for cardiac troponin T, Microchem. J. 109 (2013) 10–15. doi:10.1016/j.microc.2012.05.033.

[37] H. Jo, H. Gu, W. Jeon, H. Youn, J. Her, S.K. Kim, J. Lee, J.H. Shin, C. Ban, Electrochemical Aptasensor of Cardiac Troponin i for the Early Diagnosis of Acute Myocardial Infarction, Anal. Chem. 87 (2015) 9869–9875. doi:10.1021/acs.analchem.5b02312.

[38] H. Jo, J. Her, H. Lee, Y.B. Shim, C. Ban, Highly sensitive amperometric detection of cardiac troponin I using sandwich aptamers and screen-printed carbon electrodes,

ACCEPTED MANUSCRIPT

Talanta. 165 (2017) 442–448. doi:10.1016/j.talanta.2016.12.091.

[39] N. Karimian, M. Vagin, M.H.A. Zavar, M. Chamsaz, A.P.F. Turner, A. Tiwari, An ultrasensitive molecularly-imprinted human cardiac troponin sensor, Biosens. Bioelectron. 50 (2013) 492–498. doi:10.1016/j.bios.2013.07.013.

[40] Y. Ma, X.L. Shen, H.S. Wang, J. Tao, J.Z. Huang, Q. Zeng, L.S. Wang, MIPs-graphene nanoplatelets-MWCNTs modified glassy carbon electrode for the determination of cardiac troponin I, Anal. Biochem. 520 (2017) 9–15. doi:10.1016/j.ab.2016.12.018.

[41] A.B. Mattos, T.A. Freitas, L.T. Kubota, R.F. Dutra, An o-aminobenzoic acid film-based immunoelectrode for detection of the cardiac troponin T in human serum, Biochem. Eng. J. 71 (2013) 97–104. doi:10.1016/j.bej.2012.12.005.

[42] A. Periyakaruppan, R.P. Gandhiraman, M. Meyyappan, J.E. Koehne, Label-free detection of cardiac troponin-I using carbon nanofiber based nanoelectrode arrays, Anal. Chem. 85 (2013) 3858–3863. doi:10.1021/ac302801z.

[43] X. Qin, Y. Dong, M. Wang, Z. Zhu, M. Li, X. Chen, D. Yang, Y. Shao, C-dots assisted synthesis of gold nanoparticles as labels to catalyze copper deposition for ultrasensitive electrochemical sensing of proteins, (2018).

[44] L.P. Rodrigues, L.F. Ferreira, A.F.G. Do Monte, A.G. Brito-Madurro, J.M. Madurro, Bioelectrode Applied to Diagnosis of Cardiac Disease, J. Nanosci. Nanotechnol. 14 (2014) 6528–6538. doi:10.1166/jnn.2014.9369.

[45] A.A. Shumkov, E. V. Suprun, S.Z. Shatinina, A. V. Lisitsa, V. V. Shumyantseva, A.I. Archakov, Gold and Silver Nanoparticles for Electrochemical Detection of Cardiac Troponin I Based on Stripping Voltammetry, Bionanoscience. 3 (2013) 216–222. doi:10.1007/s12668-013-0090-9.

[46] B.V.M. Silva, I.T. Cavalcanti, M.M.S. Silva, R.F. Dutra, A carbon nanotube screen-printed electrode for label-free detection of the human cardiac troponin T, Talanta. 117 (2013) 431–437. doi:10.1016/j.talanta.2013.08.059.

[47] B.V.M. Silva, B.A.G. Rodríguez, G.F. Sales, M.D.P.T. Sotomayor, R.F. Dutra, An ultrasensitive human cardiac troponin T graphene screen-printed electrode based on electropolymerized-molecularly imprinted conducting polymer, Biosens. Bioelectron. 77 (2016) 978–985. doi:10.1016/j.bios.2015.10.068.

[48] S. Singal, A.K. Srivastava, A.M. Biradar, A. Mulchandani, Rajesh, Pt nanoparticles-chemical vapor deposited graphene composite based immunosensor for the detection of human cardiac troponin i, Sensors Actuators, B Chem. 205 (2014) 363–370. doi:10.1016/j.snb.2014.08.088.

[49] M. Szymanski, R. Porter, Electrochemical Immunoassay for Cardiac Markers With Magnetic Particles As a Solid Phase and Silver Nanoparticles As an Electroactive Bio-Label, (2009) 1738–1743.

[50] Y. Xu, S. Yang, W. Shi, Fabrication of an immunosensor for cardiac troponin I determination, Int. J. Electrochem. Sci. 12 (2017) 7931–7940. doi:10.20964/2017.09.65.

[51] N. Zanato, L. Talamini, E. Zapp, D. Brondani, I.C. Vieira, Label-free Electrochemical Immunosensor for Cardiac Troponin T Based on Exfoliated Graphite Nanoplatelets Decorated with Gold Nanoparticles, Electroanalysis. 29 (2017) 1820–1827. doi:10.1002/elan.201700157.

ACCEPTED MANUSCRIPT

[52] N. Singh, M.A. Ali, P. Rai, A. Sharma, B.D. Malhotra, R. John, Microporous nanocomposite enabled microfluidic biochip for cardiac biomarker detection, ACS Appl. Mater. Interfaces. 9 (2017) 33576–33588. doi:10.1021/acsami.7b07590.

[53] Z. Li, K. Ma, Z. Cheng, C. Yan, G. Liu, Fabrication of electrochemical immunosensor for cardiac biomarker troponin I determination and its potential for acute myocardial infarction diagnosis, Int. J. Electrochem. Sci. 12 (2017) 2389–2399. doi:10.20964/2017.03.12.

[54] E. Zapp, P.S. Da Silva, E. Westphal, H. Gallardo, A. Spinelli, I.C. Vieira, Troponin T Immunosensor Based on Liquid Crystal and Silsesquioxane-Supported Gold Nanoparticles, Bioconjug. Chem. 25 (2014) 1638–1643. doi:10.1021/bc500341a.

[55] M. Xiong, X. Wang, Y. Kong, B. Han, Development of cardiac troponin I electrochemical impedance immunosensor, Int. J. Electrochem. Sci. 12 (2017) 4204–4214. doi:10.20964/2017.05.22.

[56] R.K. Gupta, A. Periyakaruppan, M. Meyyappan, J.E. Koehne, Label-free detection of C-reactive protein using a carbon nanofiber based biosensor, Biosens. Bioelectron. 59 (2014) 112–119. doi:10.1016/j.bios.2014.03.027.

[57] A.J. Matas, K.J. Gillingham, W.D. Payne, J.S. Najarian, M.B. Pepys, G.M. Hirschfield, V. Nickeleit, M.J. Mihatsch, S.B. Schwedler, H.-U. Meier-Kriesche, S. Li, R.W.G. Gruessner, J.J. Fung, R.T. Bustami, M.L. Barr, A.B. Leichtman, S.U. Eisenhardt, J. Habersberger, A. Murphy, Y.C. Chen, K.J. Woollard, N. Bassler, H. Qian, C. Von Zur Muhlen, C.E. Hagemeyer, I. Ahrens, J. Chin-Dusting, A. Bobik, K. Peter, B. Pomahac, J. Pribaz, E. Eriksson, E.M. Bueno, J.R. Diaz-Siso, F.J. Rybicki, D.J. Annino, D. Orgill, E.J. Caterson, S. a. Caterson, M.J. Carty, Y.S. Chun, C.E. Sampson, J.E. Janis, D.S. Alam, A. Saavedra, J. a. Molnar, T. Edrich, F.M. Marty, S.G. Tullius, E.M. Bueno, G.C. Sisk, M. Francisco, B. Pomahac, S.G. Tullius, D. Braig, B. Kaiser, J.R. Thiele, H. Bannasch, K. Peter, G.B.B. Stark, H.-G. Koch, S.U. Eisenhardt, J. Habersberger, D. Braig, Y. Schmidt, K. Goerendt, V. Maurer, H. Bannasch, A. Scheichl, K.J. Woollard, E. von Dobschütz, F. Kolodgie, R. Virmani, G.B.B. Stark, K. Peter, S.U. Eisenhardt, M.H. Oberbarnscheidt, Q. Zeng, Q. Li, H. Dai, A.L. Williams, W.D. Shlomchik, D.M. Rothstein, F.G. Lakkis, Dissociation of pentameric to monomeric C-reactive protein on activated platelets localizes inflammation to atherosclerotic plaques, Circulation. 366 (2014) 857–859. doi:10.1172/JCI200318921.Introduction.

[58] V.M. Miller, M.M. Redfield, J.P. McConnell, Use of BNP and CRP as biomarkers in assessing cardiovascular disease: diagnosis versus risk., Curr. Vasc. Pharmacol. 5 (2007) 15–25. doi:10.2174/157016107779317251.

[59] N.D. Mygind, M.J. Harutyunyan, A.B. Mathiasen, R.S. Ripa, J.J. Thune, J.P. Gøtze, J.S. Johansen, J. Kastrup, The influence of statin treatment on the inflammatory biomarkers YKL-40 and HsCRP in patients with stable coronary artery disease, Inflamm. Res. 60 (2011) 281–287. doi:10.1007/s00011-010-0266-5.

[60] A.J.G. Lemos, R.P.A. Balvedi, V.R. Rodovalho, L.O. Resende, A.C.H. Castro, S. Cuadros-Orellana, J.M. Madurro, A.G. Brito-Madurro, Immunosensor assembled on polymeric nanostructures for clinical diagnosis of C-reactive protein, Microchem. J. 133 (2017) 572–576. doi:10.1016/j.microc.2017.04.026.

[61] S. Singal, A.M. Biradar, A. Mulchandani, Rajesh, Ultrasensitive Electrochemical Immunosensor Based on Pt Nanoparticle–Graphene Composite, Appl. Biochem.

ACCEPTED MANUSCRIPT

Biotechnol. 174 (2014) 971–983. doi:10.1007/s12010-014-0933-z.

[62] S. Centi, L.B. Sanmartin, S. Tombelli, I. Palchetti, M. Mascini, Detection of C reactive protein (CRP) in serum by an electrochemical aptamer-based sandwich assay, Electroanalysis. 21 (2009) 1309–1315. doi:10.1002/elan.200804560.

[63] C. Kokkinos, M. Prodromidis, A. Economou, P. Petrou, S. Kakabakos, Disposable integrated bismuth citrate-modified screen-printed immunosensor for ultrasensitive quantum dot-based electrochemical assay of C-reactive protein in human serum, Anal. Chim. Acta. 886 (2015) 29–36. doi:10.1016/j.aca.2015.05.035.

[64] S.K. Mishra, R. Pasricha, A.M. Biradar, Rajesh, ZnS-nanocrystals/polypyrrole nanocomposite film based immunosensor, Appl. Phys. Lett. 100 (2012). doi:10.1063/1.3681580.

[65] A.K. Yagati, J.C. Pyun, J. Min, S. Cho, Label-free and direct detection of C-reactive protein using reduced graphene oxide-nanoparticle hybrid impedimetric sensor, Bioelectrochemistry. 107 (2016) 37–44. doi:10.1016/j.bioelechem.2015.10.002.

[66] Z.H. Ibupoto, N. Jamal, K. Khun, M. Willander, Development of a disposable potentiometric antibody immobilized ZnO nanotubes based sensor for the detection of C-reactive protein, Sensors Actuators, B Chem. 166–167 (2012) 809–814. doi:10.1016/j.snb.2012.03.083.

[67] M. Buch, J. Rishpon, An electrochemical immunosensor for C-reactive protein based on multi-walled carbon nanotube-modified electrodes, Electroanalysis. 20 (2008) 2592–2594. doi:10.1002/elan.200804358.

[68] L. Anicai, C. Stoica, C. Vladut, A. Negru, J. Teulon, M. Odorico, Synthesis and Characterization of a Novel Screen-Printed Modified Gold Electrode with Applications in Uranyl Ions Detection Synthesis and Characterization of a Novel Screen-Printed Modified Gold Electrode with Applications in Uranyl Ions Detection, (2015).

[69] G. Bing, Xuehua, Wang, Label Free C-reactive Protein Detection Based on An Electrochemical Sensor for Clinical Application, Int. J. Electrochem. Sci. 12 (2017) 6304–6314. doi:10.20964/2017.07.60.

[70] T. Bryan, X. Luo, P.R. Bueno, J.J. Davis, An optimised electrochemical biosensor for the label-free detection of C-reactive protein in blood, Biosens. Bioelectron. 39 (2013) 94–98. doi:10.1016/j.bios.2012.06.051.

[71] W.M. Fakanya, I.E. Tothill, Detection of the inflammation biomarker C-reactive protein in serum samples: Towards an optimal biosensor formula, Biosensors. 4 (2014) 340–357. doi:10.3390/bios4040340.

[72] T. Goda, M. Toya, A. Matsumoto, Y. Miyahara, Poly(3,4-ethylenedioxythiophene) Bearing Phosphorylcholine Groups for Metal-Free, Antibody-Free, and Low-Impedance Biosensors Specific for C-Reactive Protein, ACS Appl. Mater. Interfaces. 7 (2015) 27440–27448. doi:10.1021/acsami.5b09325.

[73] I. Hafaiedh, H. Chammem, A. Abdelghani, E. Ait, L. Feldman, O. Meilhac, L. Mora, Supported protein G on gold electrode: Characterization and immunosensor application, Talanta. 116 (2013) 84–90. doi:10.1016/j.talanta.2013.04.059.

[74] H. Hennessey, N. Afara, S. Omanovic, A.L. Padjen, Electrochemical investigations of the interaction of C-reactive protein (CRP) with a CRP antibody chemically immobilized

ACCEPTED MANUSCRIPT

on a gold surface, Anal. Chim. Acta. 643 (2009) 45–53. doi:10.1016/j.aca.2009.04.009.

[75] V. Kamakoti, N.R. Shanmugam, A.S. Tanak, B. Jagannath, S. Prasad, Investigation of molybdenum-crosslinker interfaces for affinity based electrochemical biosensing applications, Appl. Surf. Sci. 436 (2018) 441–450. doi:10.1016/j.apsusc.2017.12.026.

[76] T.H. Kim, K. Abi-Samra, V. Sunkara, D.-K. Park, M. Amasia, N. Kim, J. Kim, H. Kim, M. Madou, Y.-K. Cho, Flow-enhanced electrochemical immunosensors on centrifugal microfluidic platforms, Lab Chip. 13 (2013) 3747. doi:10.1039/c3lc50374g.

[77] K.C. Lin, V. Kunduru, M. Bothara, K. Rege, S. Prasad, B.L. Ramakrishna, Biogenic nanoporous silica-based sensor for enhanced electrochemical detection of cardiovascular biomarkers proteins, Biosens. Bioelectron. 25 (2010) 2336–2342. doi:10.1016/j.bios.2010.03.032.

[78] U. Mic, V. Sunkara, H. Kim, M. Mado, B. En, M.E. Team, Fully Integrated Centrifugal microfluidic platform for electrochemical biomarker detection, 15th International Conference on Miniaturized Systems for Chemistry and Life Sciences, (2011) 1668–1670.

[79] S.K. Mishra, V. Sharma, D. Kumar, Rajesh, Biofunctionalized Gold Nanoparticle-Conducting Polymer Nanocomposite Based Bioelectrode for CRP Detection, Appl. Biochem. Biotechnol. 174 (2014) 984–997. doi:10.1007/s12010-014-0984-1.

[80] S.K. Mishra, A.K. Srivastava, D. Kumar, A. Mulchandani, Rajesh, Protein functionalized Pt nanoparticles-conducting polymer nanocomposite film: Characterization and immunosensor application, Polym. (United Kingdom). 55 (2014) 4003–4011. doi:10.1016/j.polymer.2014.05.061.

[81] N. Puri, V.K. Tanwar, V. Sharma, T. Ahuja, A.M. Biradar, Rajesh, Electrochemical characterization of surface modified gold electrode for the detection of C-reactive protein, Int. J. Integr. Biol. 9 (2010) 1–5.

[82] Rajesh, S. Singal, R.K. Kotnala, Single Frequency Impedance Analysis on Reduced Graphene Oxide Screen-Printed Electrode for Biomolecular Detection, Appl. Biochem. Biotechnol. 183 (2017) 672–683. doi:10.1007/s12010-017-2510-8.

[83] L.O. Resende, A.C.H. de Castro, A.O. Andrade, J.M. Madurro, A.G. Brito-Madurro, Immunosensor for electrodetection of the C-reactive protein in serum, J. Solid State Electrochem. (2017) 1–8. doi:10.1007/s10008-017-3820-z.

[84] A. Santos, J.P. Piccoli, N.A. Santos-Filho, E.M. Cilli, P.R. Bueno, Redox-tagged peptide for capacitive diagnostic assays, Biosens. Bioelectron. 68 (2015) 281–287. doi:10.1016/j.bios.2014.12.059.

[85] T. Songjaroen, R.M. Feeny, M.M. Mensack, W. Laiwattanapaisal, C.S. Henry, Label-free detection of C-reactive protein using an electrochemical DNA immunoassay, Sens. Bio-Sensing Res. 8 (2016) 14–19. doi:10.1016/j.sbsr.2016.03.003.

[86] X. Tan, L. Zhang, X. Deng, L. Miao, H. Li, G. zheng, Redox active molybdophosphate produced by $Cu_3(PO_4)_2$ nanospheres for enhancing enzyme-free electrochemical immunoassay of C-reactive protein, New J. Chem. 41 (2017) 11867–11871. doi:10.1039/C7NJ02629C.

[87] K. Vattipalli, K.C. Lin, B.L. Ramakrishna, S. Prasad, Enhanced electrochemical detection of cardiovascular biomarker proteins using biogenic nanoporous silica

ACCEPTED MANUSCRIPT

diatoms, Proc. IEEE Conf. Nanotechnol. (2011) 237–240. doi:10.1109/NANO.2011.6144413.

[88] V. Vermeeren, L. Grieten, N. Vanden Bon, N. Bijnens, S. Wenmackers, S.D. Janssens, K. Haenen, P. Wagner, L. Michiels, Impedimetric, diamond-based immmunosensor for the detection of C-reactive protein, Sensors Actuators, B Chem. 157 (2011) 130–138. doi:10.1016/j.snb.2011.03.037.

[89] J. Wang, J. Guo, J. Zhang, W. Zhang, Y. Zhang, RNA aptamer-based electrochemical aptasensor for C-reactive protein detection using functionalized silica microspheres as immunoprobes, Biosens. Bioelectron. 95 (2017) 100–105. doi:10.1016/j.bios.2017.04.014.

[90] Z. Yang, Y. Liu, C. Lei, X. cheng Sun, Y. Zhou, A flexible giant magnetoimpedance-based biosensor for the determination of the biomarker C-reactive protein, Microchim. Acta. 182 (2015) 2411–2417. doi:10.1007/s00604-015-1587-4.

[91] G. Yuan, C. Yu, C. Xia, L. Gao, W. Xu, W. Li, J. He, A simultaneous electrochemical multianalyte immunoassay of high sensitivity C-reactive protein and soluble CD40 ligand based on reduced graphene oxide-tetraethylene pentamine that directly adsorb metal ions as labels, Biosens. Bioelectron. 72 (2015) 237–246. doi:10.1016/j.bios.2015.04.088.

[92] J. Zhang, W. Zhang, J. Guo, J. Wang, Y. Zhang, Electrochemical detection of C-reactive protein using Copper nanoparticles and hybridization chain reaction amplifying signal, Anal. Biochem. 539 (2017) 1–7. doi:10.1016/j.ab.2017.09.017.

[93] N. Zhang, Z.Y. Ma, Y.F. Ruan, W.W. Zhao, J.J. Xu, H.Y. Chen, Simultaneous Photoelectrochemical Immunoassay of Dual Cardiac Markers Using Specific Enzyme Tags: A Proof of Principle for Multiplexed Bioanalysis, Anal. Chem. 88 (2016) 1990–1994. doi:10.1021/acs.analchem.5b04579.

[94] X. Zhang, R. Hu, K. Zhang, R. Bai, D. Li, Y. Yang, An ultrasensitive label-free immunoassay for C-reactive protein detection in human serum based on electron transfer, Anal. Methods. 8 (2016) 6202–6207. doi:10.1039/C6AY01464J.

[95] F. Zhou, M. Lu, W. Wang, Z.P. Bian, J.R. Zhang, J.J. Zhu, Electrochemical immunosensor for simultaneous detection of dual cardiac markers based on a poly(dimethylsiloxane)-gold nanoparticles composite microfluidic chip: A proof of principle, Clin. Chem. 56 (2010) 1701–1707. doi:10.1373/clinchem.2010.147256.

[96] C. Popa, M.G. Netea, P.L.C.M. van Riel, J.W.M. van der Meer, A.F.H. Stalenhoef, The role of TNF-α in chronic inflammatory conditions, intermediary metabolism, and cardiovascular risk, J. Lipid Res. 48 (2007) 751–762. doi:10.1194/jlr.R600021-JLR200.

[97] D.E. Moller, Potential Role of TNF-α in the Pathogenesis of Insulin Resistance and Type 2 Diabetes, Trends Endocrinol. Metab. 11 (2000) 212–217. doi:10.1016/S1043-2760(00)00272-1.

[98] Y. Liu, T. Kwa, A. Revzin, Simultaneous detection of cell-secreted TNF-α and IFN-γ using micropatterned aptamer-modified electrodes, Biomaterials. 33 (2012) 7347–7355. doi:10.1016/j.biomaterials.2012.06.089.

[99] R. Pruna, F. Palacio, A. Baraket, N. Zine, A. Streklas, J. Bausells, A. Errachid, M. López, A low-cost and miniaturized potentiostat for sensing of biomolecular species such as

ACCEPTED MANUSCRIPT

ACCEPTED MANUSCRIPT

TNF-α by electrochemical impedance spectroscopy, Biosens. Bioelectron. 100 (2018) 533–540. doi:10.1016/j.bios.2017.09.049.

[100] S.K. Arya, P. Estrela, Electrochemical immunosensor for tumor necrosis factor-alpha detection in undiluted serum, Methods. 116 (2017) 125–131. doi:10.1016/j.ymeth.2016.12.001.

[101] M. Mazloum-Ardakani, L. Hosseinzadeh, A. Khoshroo, Label-free electrochemical immunosensor for detection of tumor necrosis factor α based on fullerene-functionalized carbon nanotubes/ionic liquid, J. Electroanal. Chem. 757 (2015) 58–64. doi:10.1016/j.jelechem.2015.09.006.

[102] P. Kongsuphol, H.H. Ng, J.P. Pursey, S.K. Arya, C.C. Wong, E. Stulz, M.K. Park, EIS-based biosensor for ultra-sensitive detection of TNF-α from non-diluted human serum, Biosens. Bioelectron. 61 (2014) 274–279. doi:10.1016/j.bios.2014.05.017.

[103] E. Sánchez-Tirado, C. Salvo, A. González-Cortés, P. Yáñez-Sedeño, F. Langa, J.M. Pingarrón, Electrochemical immunosensor for simultaneous determination of interleukin-1 beta and tumor necrosis factor alpha in serum and saliva using dual screen printed electrodes modified with functionalized double–walled carbon nanotubes, Anal. Chim. Acta. 959 (2017) 66–73. doi:10.1016/j.aca.2016.12.034.

[104] T. Li, Z. Si, L. Hu, H. Qi, M. Yang, Prussian Blue-functionalized ceria nanoparticles as label for ultrasensitive detection of tumor necrosis factor-α, Sensors Actuators, B Chem. 171–172 (2012) 1060–1065. doi:10.1016/j.snb.2012.06.034.

[105] M. Mazloum-Ardakani, L. Hosseinzadeh, A. Khoshroo, Ultrasensitive Electrochemical Immunosensor for Detection of Tumor Necrosis Factor- α Based on Functionalized MWCNT-Gold Nanoparticle/Ionic Liquid Nanocomposite, Electroanalysis. 27 (2015) 2518–2526. doi:10.1002/elan.201500104.

[106] L. Li, M. Li, W. Wang, Q. Zhang, D. Liu, X. Li, H. Jiang, High sensitivity determination of TNF-α for early diagnosis of neonatal infections with a novel and reusable electrochemical sensor, Sensors (Switzerland). 17 (2017). doi:10.3390/s17050992.

[107] I.R. Comnea-Stancu, R.-I. Stefan-van Staden, A.R. Biris, A Graphene Stochastic Sensor for the Molecular Screening of TNF-α, J. Electrochem. Soc. 162 (2015) B245–B247. doi:10.1149/2.0931509jes.

[108] M. Mazloum-Ardakani, L. Hosseinzadeh, A Sensitive Electrochemical Aptasensor for TNF-α Based on Bimetallic Ag@Pt Core-Shell Nanoparticle Functionalized Graphene Nanostructures as Labels for Signal Amplification, J. Electrochem. Soc. 163 (2016) B119–B124. doi:10.1149/2.0241605jes.

[109] M. Mazloum-Ardakani, L. Hosseinzadeh, Highly-sensitive label-free immunosensor for tumor necrosis factor α based on Ag@Pt core–shell nanoparticles supported on MWCNTs as an efficient electrocatalyst nanocomposite, RSC Adv. 5 (2015) 70781–70786. doi:10.1039/C5RA08016A.

[110] R.-I. Stefan-van Staden, I.R. Comnea-Stancu, C.A. Visan, A. Streinu-Cercel, Diamond Paste-Based Stochastic Sensor for Screening of Children's Cerebrospinal Fluid, J. Electrochem. Soc. 162 (2015) B351–B353. doi:10.1149/2.0741514jes.

[111] Z. Sun, L. Deng, H. Gan, R. Shen, M. Yang, Y. Zhang, Sensitive immunosensor for tumor necrosis factor α based on dual signal amplification of ferrocene modified self-

ACCEPTED MANUSCRIPT

assembled peptide nanowire and glucose oxidase functionalized gold nanorod, Biosens. Bioelectron. 39 (2013) 215–219. doi:10.1016/j.bios.2012.07.050.

[112] Z. Yin, Y. Liu, L.P. Jiang, J.J. Zhu, Electrochemical immunosensor of tumor necrosis factor- α based on alkaline phosphatase functionalized nanospheres, Biosens. Bioelectron. 26 (2011) 1890–1894. doi:10.1016/j.bios.2010.03.025.

[113] S. Weng, M. Chen, C. Zhao, A. Liu, L. Lin, Q. Liu, J. Lin, X. Lin, Label-free electrochemical immunosensor based on K3[Fe(CN)6] as signal for facile and sensitive determination of tumor necrosis factor-alpha, Sensors Actuators, B Chem. 184 (2013) 1–7. doi:10.1016/j.snb.2013.03.141.

[114] L. Liu, F. Liu, D. Jiang, G. Xiang, C. Liu, J. Yang, X. Pu, Hybridization chain reaction and target recycling enhanced tumor necrosis factor alpha aptasensor with host-guest interaction for signal probe collection, Sensors Actuators, B Chem. 231 (2016) 680–687. doi:10.1016/j.snb.2016.03.098.

[115] Y. Hou, T. Li, H. Huang, H. Quan, X. Miao, M. Yang, Electrochemical immunosensor for the detection of tumor necrosis factor α based on hydrogel prepared from ferrocene modified amino acid, Sensors Actuators, B Chem. 182 (2013) 605–609. doi:10.1016/j.snb.2013.03.067.

[116] T.S. Pui, P. Kongsuphol, S.K. Arya, T. Bansal, Detection of tumor necrosis factor (TNF-α) in cell culture medium with label free electrochemical impedance spectroscopy, Sensors Actuators, B Chem. 181 (2013) 494–500. doi:10.1016/j.snb.2013.02.019.

[117] M. Mazloum-Ardakani, L. Hosseinzadeh, Z. Taleat, Synthesis and electrocatalytic effect of Ag@Pt core-shell nanoparticles supported on reduced graphene oxide for sensitive and simple label-free electrochemical aptasensor, Biosens. Bioelectron. 74 (2015) 30–36. doi:10.1016/j.bios.2015.05.072.

[118] A. Longo, A. Baraket, M. Vatteroni, N. Zine, J. Baussells, R. Fuoco, F. Di Francesco, G.S. Karanasiou, D.I. Fotiadis, A. Menciassi, A. Errachid, Highly Sensitive Electrochemical BioMEMS for TNF-α Detection in Humansaliva: Heart Failure, Procedia Eng. 168 (2016) 97–100. doi:10.1016/j.proeng.2016.11.156.

[119] Y. Liu, Q. Zhou, A. Revzin, An aptasensor for electrochemical detection of tumor necrosis factor in human blood, Analyst. 138 (2013) 4321. doi:10.1039/c3an00818e.

[120] G. Baydemir, F. Bettazzi, I. Palchetti, D. Voccia, Strategies for the development of an electrochemical bioassay for TNF-alpha detection by using a non-immunoglobulin bioreceptor, Talanta. 151 (2016) 141–147. doi:10.1016/j.talanta.2016.01.021.

[121] I.D. Iala, S.S. Ato, M.U. Sui, K.N. Akashima, T.N. Ishihara, S.T. Akenaka, Advancements in Instrumentation Development of a Membrane-based Microwave-mediated Electrochemical ELISA Method for TNF- α Detection in Patients with Periodontitis, 29 (2013) 927–930. doi:10.2116/analsci.29.927.

[122] S.K. Arya, P. Kongsuphol, M.K. Park, On-chip electrochemical immunoassay platform for specific protein biomarker estimation in undiluted serum using off-surface membrane matrix, Biosens. Bioelectron. 91 (2017) 721–727. doi:10.1016/j.bios.2017.01.033.

[123] P. Kongsuphol, G.C.F. Lee, S.K. Arya, S.Y. Chiam, M.K. Park, Miniaturized electrophoresis electrochemical protein sensor (MEEPS) for multiplexed protein detections, Sensors Actuators, B Chem. 244 (2017) 823–830.

ACCEPTED MANUSCRIPT

doi:10.1016/j.snb.2017.01.026.

[124] E.B. Aydın, M. Aydın, M.K. Sezgintürk, A highly sensitive immunosensor based on ITO thin films covered by a new semi-conductive conjugated polymer for the determination of TNFα in human saliva and serum samples, Biosens. Bioelectron. 97 (2017) 169–176. doi:10.1016/j.bios.2017.05.056.

[125] F.G. Bellagambi, A. Baraket, A. Longo, M. Vatteroni, N. Zine, J. Bausells, R. Fuoco, F. Di Francesco, P. Salvo, G.S. Karanasiou, D.I. Fotiadis, A. Menciassi, A. Errachid, Electrochemical biosensor platform for TNF-α cytokines detection in both artificial and human saliva: Heart failure, Sensors Actuators, B Chem. 251 (2017) 1026–1033. doi:10.1016/j.snb.2017.05.169.

[126] Y. Liu, Y. Liu, Z. Matharu, A. Rahimian, A. Revzin, Detecting multiple cell-secreted cytokines from the same aptamer-functionalized electrode, Biosens. Bioelectron. 64 (2015) 43–50. doi:10.1016/j.bios.2014.08.034.

[127] U. Eletxigerra, J. Martinez-perdiguero, S. Merino, R. Villalonga, Analytica Chimica Acta Amperometric magnetoimmunoassay for the direct detection of tumor necrosis factor alpha biomarker in human serum, Anal. Chim. Acta. 838 (2014) 37–44. doi:10.1016/j.aca.2014.05.047.

[128] N. Puri, A. Niazi, A.K. Srivastava, Rajesh, Biointerfacial impedance characterization of reduced graphene oxide supported carboxyl pendant conducting copolymer based electrode, Electrochim. Acta. 123 (2014) 211–218. doi:10.1016/j.electacta.2013.12.188.

[129] T.M. O'Regan, L.J. O'Riordan, M. Pravda, C.K. O'Sullivan, G.G. Guilbault, Direct detection of myoglobin in whole blood using a disposable amperometric immunosensor, Anal. Chim. Acta. 460 (2002) 141–150. doi:10.1016/S0003-2670(02)00230-1.

[130] S.S. Mandal, K.K. Narayan, A.J. Bhattacharyya, Employing denaturation for rapid electrochemical detection of myoglobin using TiO2 nanotubes, J. Mater. Chem. B. 1 (2013) 3051. doi:10.1039/c3tb20409j.

[131] M. Szymanski, A.P.F. Turner, R. Porter, Electrochemical dissolution of silver nanoparticles and its application in metalloimmunoassay, Electroanalysis. 22 (2010) 191–198. doi:10.1002/elan.200900275.

[132] X. Ren, Y. Zhang, Y. Sun, L. Gao, Development of electrochemical impedance immunosensor for sensitive determination of myoglobin, Int. J. Electrochem. Sci. 12 (2017) 7765–7776. doi:10.20964/2017.08.18.

[133] J.A. Ribeiro, C.M. Pereira, A.F. Silva, M.G.F. Sales, Electrochemical detection of cardiac biomarker myoglobin using polyphenol as imprinted polymer receptor, Anal. Chim. Acta. 981 (2017) 41–52. doi:10.1016/j.aca.2017.05.017.

[134] Y.-W. Liu, Q.-F. Yang, P.-Y. Zuo, C.-L. Xiao, X.-L. Chen, and C.-Y. Liu: Elevated Serum Levels of Soluble Axl in Acute Coronary Syndrome. *The American Journal of the Medical Sciences* 349 (2015) 124.

[135] M. Batlle, P. Recarte-Pelz, E. Roig, M. A. Castel, M. Cardona, M. Farrero, J. T. Ortiz, B. Campos, M. J. Pulgarín, J. Ramírez, F. Pérez-Villa, and P. García de Frutos: AXL receptor tyrosine kinase is increased in patients with heart failure. *International Journal*

ACCEPTED MANUSCRIPT

of Cardiology **173**, 402 (2014).

[136] L. Sun, W. Li, M. Wang, W. Ding, Y. Ji, Development of an electrochemical impedance immunosensor for myoglobin determination, Int. J. Electrochem. Sci. 12 (2017) 6170–6179. doi:10.20964/2017.07.72.

[137] D. Sharma, J. Lee, H. Shin, An electrochemical immunosensor based on a 3D carbon system consisting of a suspended mesh and substrate-bound interdigitated array nanoelectrodes for sensitive cardiac biomarker detection, Biosens. Bioelectron. 107 (2018) 10–16. doi:10.1016/j.bios.2018.02.010.

[138] R. Khan, M. Pal, A. V. Kuzikov, T. Bulko, E. V. Suprun, V. V. Shumyantseva, Impedimetric immunosensor for detection of cardiovascular disorder risk biomarker, Mater. Sci. Eng. C. 68 (2016) 52–58. doi:10.1016/j.msec.2016.05.107.

[139] B. Zhang, Y. Zhang, W. Liang, X. Yu, H. Tan, G. Wang, A. Li, J. Jin, L. Huang, Copper sulfide-functionalized molybdenum disulfide nanohybrids as nanoenzyme mimics for electrochemical immunoassay of myoglobin in cardiovascular disease, RSC Adv. 7 (2017) 2486–2493. doi:10.1039/C6RA26372K.

[140] C. Li, J. Li, X. Yang, L. Gao, L. Jing, X. Ma, A label-free electrochemical aptasensor for sensitive myoglobin detection in meat, Sensors Actuators, B Chem. 242 (2017) 1239–1245. doi:10.1016/j.snb.2016.09.087.

[141] G. Zhang, Z. Liu, L. Wang, Y. Guo, Electrochemical aptasensor for myoglobin-specific recognition based on porphyrin functionalized graphene-conjugated gold nanocomposites, Sensors (Switzerland). 16 (2016). doi:10.3390/s16111803.

[142] N. Puri, S.K. Mishra, A. Niazi, A.K. Srivastava, Rajesh, Physicochemical characteristics of reduced graphene oxide based Pt-nanoparticles-conducting polymer nanocomposite film for immunosensor applications, J. Chem. Technol. Biotechnol. 90 (2015) 1699–1706. doi:10.1002/jctb.4480.

[143] H.Y.L. Ee, J.S.C. Hoi, P.G. Uruprasath, B.L. Ee, An Electrochemical Biosensor Based on a Myoglobin-specific Binding Peptide for Early Diagnosis of Acute Myocardial Infarction, 31 (2015) 699–704.

[144] Y. Wang, M. Han, X. Ye, K. Wu, T. Wu, C. Li, Voltammetric myoglobin sensor based on a glassy carbon electrode modified with a composite film consisting of carbon nanotubes and a molecularly imprinted polymerized ionic liquid, Microchim. Acta. 184 (2017) 195–202. doi:10.1007/s00604-016-2005-2.

[145] S.M. Taghdisi, N.M. Danesh, M. Ramezani, A.S. Emrani, K. Abnous, A novel electrochemical aptasensor based on Y-shape structure of dual-aptamer-complementary strand conjugate for ultrasensitive detection of myoglobin, Biosens. Bioelectron. 80 (2016) 532–537. doi:10.1016/j.bios.2016.02.029.

[146] F.T.C. Moreira, R.A.F. Dutra, J.P.C. Noronha, M.G.F. Sales, Electrochemical biosensor based on biomimetic material for myoglobin detection, Electrochim. Acta. 107 (2013) 481–487. doi:10.1016/j.electacta.2013.06.061.

[147] F.T.C. Moreira, S. Sharma, R.A.F. Dutra, J.P.C. Noronha, A.E.G. Cass, M.G.F. Sales, Smart plastic antibody material (SPAM) tailored on disposable screen printed electrodes

ACCEPTED MANUSCRIPT

for protein recognition: Application to myoglobin detection, Biosens. Bioelectron. 45 (2013) 237–244. doi:10.1016/j.bios.2013.02.012.

[148] F.T.C. Moreira, S. Sharma, R.A.F. Dutra, J.P.C. Noronha, A.E.G. Cass, M.G.F. Sales, Protein-responsive polymers for point-of-care detection of cardiac biomarker, Sensors Actuators, B Chem. 196 (2014) 123–132. doi:10.1016/j.snb.2014.01.038.

[149] S.K. Tuteja, R. Chen, M. Kukkar, C.K. Song, R. Mutreja, S. Singh, A.K. Paul, H. Lee, K.H. Kim, A. Deep, C.R. Suri, A label-free electrochemical immunosensor for the detection of cardiac marker using graphene quantum dots (GQDs), Biosens. Bioelectron. 86 (2016) 548–556. doi:10.1016/j.bios.2016.07.052.

[150] V. V. Shumyantseva, T. V. Bulko, L. V. Sigolaeva, A. V. Kuzikov, P. V. Pogodin, A.I. Archakov, Molecular imprinting coupled with electrochemical analysis for plasma samples classification in acute myocardial infarction diagnostic, Biosens. Bioelectron. 99 (2018) 216–222. doi:10.1016/j.bios.2017.07.026.

[151] V. Shumyantseva, E. Suprun, T. Bulko, A. Archakov, Electrochemical methods for the investigation of bioaffinity interactions based on gold nanoparticles modified sensors, Electroanalysis. 21 (2009) 530–535. doi:10.1002/elan.200804439.

[152] S.K. Mishra, A.K. Srivastava, D. Kumar, A.M. Biradar, Rajesh, Microstructural and electrochemical impedance characterization of bio-functionalized ultrafine ZnS nanocrystals–reduced graphene oxide hybrid for immunosensor applications, Nanoscale. 5 (2013) 10494. doi:10.1039/c3nr02575f.

[153] I. Lee, X. Luo, X.T. Cui, M. Yun, Highly sensitive single polyaniline nanowire biosensor for the detection of immunoglobulin G and myoglobin, Biosens. Bioelectron. 26 (2011) 3297–3302. doi:10.1016/j.bios.2011.01.001.

[154] V. Kumar, J.R. Brent, M. Shorie, H. Kaur, G. Chadha, A.G. Thomas, E.A. Lewis, A.P. Rooney, L. Nguyen, X.L. Zhong, M.G. Burke, S.J. Haigh, A. Walton, P.D. McNaughter, A.A. Tedstone, N. Savjani, C.A. Muryn, P. O'Brien, A.K. Ganguli, D.J. Lewis, P. Sabherwal, Nanostructured aptamer-functionalized black phosphorus sensing platform for label-free detection of myoglobin, a cardiovascular disease biomarker, ACS Appl. Mater. Interfaces. 8 (2016) 22860–22868. doi:10.1021/acsami.6b06488.

[155] S.K. Mishra, A.K. Srivastava, D. Kumar, R. Rajesh, Bio-functionalized Pt nanoparticles based electrochemical impedance immunosensor for human cardiac myoglobin, RSC Adv. 4 (2014) 21267–21276. doi:10.1039/C4RA00105B.

[156] V. Kumar, M. Shorie, A.K. Ganguli, P. Sabherwal, Graphene-CNT nanohybrid aptasensor for label free detection of cardiac biomarker myoglobin, Biosens. Bioelectron. 72 (2015) 56–60. doi:10.1016/j.bios.2015.04.089.

[157] S. Singh, S.K. Tuteja, D. Sillu, A. Deep, C.R. Suri, Gold nanoparticles-reduced graphene oxide based electrochemical immunosensor for the cardiac biomarker myoglobin, Microchim. Acta. 183 (2016) 1729–1738. doi:10.1007/s00604-016-1803-x.

[158] S.K. Mishra, D. Kumar, A.M. Biradar, Rajesh, Electrochemical impedance spectroscopy characterization of mercaptopropionic acid capped ZnS nanocrystal based bioelectrode for the detection of the cardiac biomarker-myoglobin, Bioelectrochemistry. 88 (2012) 118–126. doi:10.1016/j.bioelechem.2012.07.006.

[159] E. Suprun, T. Bulko, A. Lisitsa, O. Gnedenko, A. Ivanov, V. Shumyantseva, A.

ACCEPTED MANUSCRIPT

Archakov, Electrochemical nanobiosensor for express diagnosis of acute myocardial infarction in undiluted plasma, Biosens. Bioelectron. 25 (2010) 1694–1698. doi:10.1016/j.bios.2009.12.009.

[160] F.T.C. Moreira, R.A.F. Dutra, J.P. Noronha, M.G.F. Sales, Novel sensory surface for creatine kinase electrochemical detection, Biosens. Bioelectron. 56 (2014) 217–222. doi:10.1016/j.bios.2013.12.052.

[161] G. Li, T. Li, Y. Deng, Y. Cheng, F. Shi, W. Sun, Z. Sun, Electrodeposited nanogold decorated graphene modified carbon ionic liquid electrode for the electrochemical myoglobin biosensor, J. Solid State Electrochem. 17 (2013) 2333–2340. doi:10.1007/s10008-013-2098-z.

[162] X. Wang, Z. You, H. Sha, Z. Sun, W. Sun, Electrochemical myoglobin biosensor based on carbon ionic liquid electrode modified with Fe3O4@SiO2 microsphere, J. Solid State Electrochem. 18 (2014) 207–213. doi:10.1007/s10008-013-2259-0.

[163] T. Geng, Z. Song, J. Zhang, Z. Xu, Creatine kinase determination based on an electrochemical impedance immunosensor, Int. J. Electrochem. Sci. 12 (2017) 8552–8563. doi:10.20964/2017.09.60.

[164] N. Puri, A. Niazi, A.K. Srivastava, Rajesh, Synthesis and Characterization of Reduced Graphene Oxide Supported Gold Nanoparticles-Poly(Pyrrole-Co-Pyrrolepropylic Acid) Nanocomposite-Based Electrochemical Biosensor, Appl. Biochem. Biotechnol. 174 (2014) 911–925. doi:10.1007/s12010-014-0997-9.

[165] X. Kong, X. Rao, J. Han, M. Wei, X. Duan, Layer-by-layer assembly of bi-protein/layered double hydroxide ultrathin film and its electrocatalytic behavior for catechol, Biosens. Bioelectron. 26 (2010) 549–554. doi:10.1016/j.bios.2010.07.045.

[166] J.F. Rusling, G. Sotzing, F. Papadimitrakopoulosa, Designing nanomaterial-enhanced electrochemical immunosensors for cancer biomarker proteins, Bioelectrochemistry. 76 (2009) 189–194. doi:10.1016/J.BIOELECHEM.2009.03.011.

[167] Z. Cao, X. Jiang, Q. Xie, S. Yao, A third-generation hydrogen peroxide biosensor based on horseradish peroxidase immobilized in a tetrathiafulvalene tetracyanoquinodimethane/multiwalled carbon nanotubes film, Biosens. Bioelectron. 24 (2008) 222–227. doi:10.1016/j.bios.2008.03.021.

[168] N. Jordanova, M. Gyöngyösi, A. Khorsand, C. Falkensammer, G. Zorn, J. Wojta, A. Anvari, K. Huber, New cut-off values of cardiac markers for risk stratification of angina pectoris., Int. J. Cardiol. 99 (2005) 429–35. doi:10.1016/j.ijcard.2004.03.003.

[169] WHO | Cardiovascular diseases (CVDs), WHO. (2017).

[170] S.A. Ozkan, B. Uslu, From mercury to nanosensors: Past, present and the future perspective of electrochemistry in pharmaceutical and biomedical analysis, J. Pharm. Biomed. Anal. 130 (2016) 126–140. doi:10.1016/j.jpba.2016.05.006.

[171] R.N. Goyal, S. Chatterjee, A.R.S. Rana, The effect of modifying an edge-plane pyrolytic graphite electrode with single-wall carbon nanotubes on its use for sensing diclofenac, Carbon N. Y. 48 (2010) 4136–4144. doi:10.1016/J.CARBON.2010.07.024.

[172] S.B. Revin, S.A. John, Electrochemical sensor for neurotransmitters at physiological pH using a heterocyclic conducting polymer modified electrode, Analyst. 137 (2012) 209–215. doi:10.1039/C1AN15746A.

ACCEPTED MANUSCRIPT

[173] N. Karadas, B. Bozal-Palabiyik, B. Uslu, S.A. Ozkan, Functionalized carbon nanotubes - with silver nanoparticles to fabricate a sensor for the determination of zolmitriptan in its dosage forms and biological samples, Sensors Actuators, B Chem. 186 (2013) 486–494. doi:10.1016/j.snb.2013.06.055.

[174] N. Karadas-Bakirhan, S. Patris, S.A. Ozkan, A. Can, J.M. Kauffmann, Determination of the Anticancer Drug Sorafenib in Serum by Adsorptive Stripping Differential Pulse Voltammetry Using a Chitosan/Multiwall Carbon Nanotube Modified Glassy Carbon Electrode, Electroanalysis. 28 (2016) 358–365. doi:10.1002/elan.201500384.

[175] J. Lei, H. Ju, Nanotubes in biosensing, Wiley Interdiscip. Rev. Nanomedicine Nanobiotechnology. 2 (2010) 496–509. doi:10.1002/wnan.94.

[176] L. Wu, X.Zhang, H. Ju, Detection of NADH and Ethanol Based on Catalytic Activity of Soluble Carbon Nanofiber with Low Overpotential, (2006). doi:10.1021/AC061282+.

[177] P. Taylor, B. Uslu, S.A. Ozkan, Electroanalytical Application of Carbon Based Electrodes to the Pharmaceuticals Electroanalytical Application of, (2007) 37–41. doi:10.1080/00032710701242121.

[178] B. Rezaei, A.M. Shoushtari, M. Rabiee, L. Uzun, W.C. Mak, A.P.F. Turner, An electrochemical immunosensor for cardiac Troponin I using electrospun carboxylated multi-walled carbon nanotube-whiskered nanofibres, Talanta. 182 (2018) 178–186. doi:10.1016/J.TALANTA.2018.01.046.

[179] F. Chekin, A. Vasilescu, R. Jijie, S.K. Singh, S. Kurungot, M. Iancu, G. Badea, R. Boukherroub, S. Szunerits, Sensitive electrochemical detection of cardiac troponin I in serum and saliva by nitrogen-doped porous reduced graphene oxide electrode, Sensors Actuators B Chem. 262 (2018) 180–187. doi:10.1016/J.SNB.2018.01.215.

[180] E.C. Dreaden, A.M. Alkilany, X. Huang, C.J. Murphy, M.A. El-Sayed, The golden age: gold nanoparticles for biomedicine., Chem. Soc. Rev. 41 (2012) 2740–79. doi:10.1039/c1cs15237h.

[181] M. Patil, F. Umanzor, R. Kormos, P.N. Kumta, Platinum aptasensor wire arrays for cardiac biomarker detection, Mater. Today Commun. 15 (2018) 55–60. doi:10.1016/J.MTCOMM.2018.02.018.

[182] J.A. Ho, H.-C. Chang, N.-Y. Shih, L.-C. Wu, Y.-F. Chang, C.-C. Chen, C. Chou, Diagnostic Detection of Human Lung Cancer-Associated Antigen Using a Gold Nanoparticle-Based Electrochemical Immunosensor, Anal. Chem. 82 (2010) 5944–5950. doi:10.1021/ac1001959.

[183] E. Zapp, E. Westphal, H. Gallardo, B. de Souza, I. Cruz Vieira, Liquid crystal and gold nanoparticles applied to electrochemical immunosensor for cardiac biomarker, Biosens. Bioelectron. 59 (2014) 127–133. doi:10.1016/J.BIOS.2014.03.026.

[184] G. Ozcelikay, B. Dogan-Topal, S.A. Ozkan, An Electrochemical Sensor Based on Silver Nanoparticles-Benzalkonium Chloride for the Voltammetric Determination of Antiviral Drug Tenofovir, Electroanalysis. (2018) 1–13. doi:10.1002/elan.201700753.

[185] N. Karadas-Bakirhan, A. Sarakbi, M. Vandeput, S.A. Ozkan, J.M. Kauffmann, Liquid Chromatography with Amperometric Detection at a Silver Based Detector for the Determination of Thiocompounds: Application to the Assay of Thiopurine Antimetabolites in Urine, Anal. Chem. 87 (2015) 6730–6735.

ACCEPTED MANUSCRIPT

doi:10.1021/acs.analchem.5b00879.

[186] G. Jie, L. Tan, Y. Zhao, X. Wang, A novel silver nanocluster in situ synthesized as versatile probe for electrochemiluminescence and electrochemical detection of thrombin by multiple signal amplification strategy, Biosens. Bioelectron. 94 (2017) 243–249. doi:10.1016/J.BIOS.2017.03.015.

[187] J.Z. Hilt, M.E. Byrne, Configurational biomimesis in drug delivery: molecular imprinting of biologically significant molecules, Adv. Drug Deliv. Rev. 56 (2004) 1599–1620. doi:10.1016/J.ADDR.2004.04.002.

[188] P.I. Mathias, T.H. Connor, C. B'Hymer, A review of high performance liquid chromatographic-mass spectrometric urinary methods for anticancer drug exposure of health care workers, J. Chromatogr. B. 1060 (2017) 316–324. doi:10.1016/J.JCHROMB.2017.06.028.

[189] H.H. Yang, S. Zhang, F. Tan, Z. Huang, X. Wang, Surface Molecularly Imprinted Nanowires for Biorecognition, J. Am. Chem. Soc., 127 (2005), 1378–1379 doi:10.1021/JA0467622.

[190] D. Elsevier Science (Firm), B.B. Prasad, Sensors and actuators. B, Chemical., Elsevier Science Pub. Co, 2012.

[191] M.I. Mohammed, M.P.Y. Desmulliez, Lab-on-a-chip based immunosensor principles and technologies for the detection of cardiac biomarkers: a review, Lab Chip. 11 (2011) 569–595. doi:10.1039/C0LC00204F.

[192] F.S. Apple, A. Falahati, P.R. Paulsen, E.A. Miller, S.W. Sharkey, Improved detection of minor ischemic myocardial injury with measurement of serum cardiac troponin I., Clin. Chem. 43 (1997) 2047–51.

[193] J.Wang, A. Ibáñez, M. P Chatrathi, A. Escarpa, Electrochemical Enzyme Immunoassays on Microchip Platforms, Anal. Chem., *73* (2001), 5323–5327. doi:10.1021/AC010808H.

[194] M.A. Grachev, L.E. Matveev, E.K. Pressman, V. V Roschke, A rapid method for myoglobin radioimmunoanalysis as a diagnostic tool in myocardial infarction., Clin. Chim. Acta. 124 (1982) 235–8.

[195] T. Olsson, K. Bergström, A. Thore, Chemiluminescent immunosorbent assay of serum myoglobin based on the luminol reaction., Clin. Chim. Acta. 138 (1984) 31–40.

[196] H. Jo, J. Her, W. Leen, H. Shim, YB. Ban, C., Highly sensitive amperometric detection of cardiac troponin I using sandwich aptamers and screen-printed carbon electrodes, Talanta 165 (2017) 442–448. 10.1016/j.talanta.2016.12.091.

[197] A.J. Bard, L.R. Faulkner, Electrochemical methods : fundamentals and applications, Wiley, 2001.

[198] R.N. Vyas, K. Li, B. Wang, Modifying Randles Circuit for Analysis of Polyoxometalate Layer-by-Layer Films, J. Phys. Chem. B. 114 (2010) 15818–15824. doi:10.1021/jp105075t.

[199] V. Bhalla, S. Carrara, P. Sharma, Y. Nangia, C. Raman Suri, Gold nanoparticles mediated label-free capacitance detection of cardiac troponin I, Sensors Actuators B Chem. 161 (2012) 761–768. doi:10.1016/J.SNB.2011.11.029.

ACCEPTED MANUSCRIPT

[200] J.H. Chua, R.-E. Chee, A. Agarwal, S.M. Wong, G.-J. Zhang, Label-Free Electrical Detection of Cardiac Biomarker with Complementary Metal-Oxide Semiconductor-Compatible Silicon Nanowire Sensor Arrays, Anal. Chem. 81 (2009) 6266–6271. doi:10.1021/ac901157x.

[201] E.A. de Vasconcelos, N.G. Peres, C.O. Pereira, V.L. da Silva, E.F. da Silva, R.F. Dutra, Potential of a simplified measurement scheme and device structure for a low cost label-free point-of-care capacitive biosensor, Biosens. Bioelectron. 25 (2009) 870–876. doi:10.1016/j.bios.2009.08.050.

ACCEPTED MANUSCRIPT

ACCEPTED MANUSCRIPT

ACCEPTED MANUSCRIPT

ACCEPTED MANUSCRIPT

Figure and Table Legends

Figure 1. Global status report on leading causes of deaths in all over the world [1].

Figure 2. Cyclic voltammetry of SPEs at different concentrations of cTnT (1.0, 2.5, 5.0 and 10 ng mL^{-1}, (a)–(d), respectively), in the presence (a) and absence (b) of the microspheres on the epoxy-based composite [5]. Reprinted from ref. [27] with permission of Elsevier.

Figure 3. (a) Nyquist plots (Z' vs. $-Z''$) obtained from (i) ITO (□), (ii) NP/ITO (○), (iii) rGO/ITO (△) and (iv) rGO-NP/ITO (◇), each in 5 mM $[Fe(CN)_6]^{3-/4-}$ solution. The solid lines represents the experimental fit results to the measured data; (a, inset) Modified Randles equivalent circuit used to fit the experimental data to extrapolate impedance parameters; (b) Bode plots obtained after various steps of the process for (i,—) rGO-NP; (ii, – – –) MPA; (iii, ⋯) EDC-NHS; (iv, −·–) for anti-CRP; (v, −··–) for BSA and (vi, - - - -) for CRP (1 μg mL^{-1}) towards developing CRP detection sensor [6]. Reprinted from ref. [60] with permission of Elsevier.

Figure 4. Electrochemical response of the PB-CeO_2 immunosensor at −0.2 V to 1 mM H_2O_2 after incubation with TNF-α of various concentrations. From a–e, 0.01, 0.05, 0.1, 0.5, 5 ng mL^{-1}. Reprinted from ref. [7] with permission of Elsevier.

Figure 5. Electrochemical evaluation in presence of 5 mM $[Fe(CN)_6]^{3-/4-}$ redox probe of template rebinding with (A) MIP and (B) NIP receptor films, after incubation in different concentrations of MYO (from 0.001 ng mL^{-1} to 100 μg mL^{-1}, in 0.1 M PBS pH 7.0) for 10 min. Reprinted from ref. [8] with permission of Elsevier.

Figure 6. Schematic view of the stepwise fabrication of immunosensor and the mechanism of detection. Reprinted from ref. [171] with permission of Elsevier.

Figure 7. (A) The synthesis proces for N-prGO; (B) XPS results for N-prGO; (C) GC responses with cyclic voltammetry (black), GC/prGO (grey), and GC/N-prGO (blue) using $[Fe(CN)_6]^{4-}$ (5 mM)/PBS (0.1 M), scan rate = 100 mV s^{-1}; (D) morphology study of GC/N-prGO via SEM**.** Reprinted from ref. [172] with permission of Elsevier.

Figure 8. (a) Equivalent circuit, (b) Nyquist plots that conducted after each step of functionalization for the biosensor (10 mg mL^{-1} cysteamine, 25% glutaraldehyde, 1 mg mL^{-1} Neutravidin, and 150 μg mL^{-1} aptamer), (c) Functionalization process (d) Nyquist plots of EIS experiments conducted after each successive concentration of BNP demonstrating an increase in charge-transfer resistance with an increase in BNP concentration, (e) Nyquist plots of EIS experiments conducted after each successive concentration of TnT demonstrating an increase in charge-transfer resistance with an increase in TnT concentration. All EIS experiments were conducted in 5 mM $(Fe(CN_6)^{3-/4-})$ in 10 mM PBS, with 5 μm polished 0.5 mm diameter platinum working electrodes, Ag wire reference electrode, and Pt wire counter electrode across 300,000 Hz–0.01 Hz at 10 mV rms AC voltage. Reprinted from ref. [174] with permission of Elsevier.

Figure 9. (A) Schematic representation of liquid crystal immunosensor surface, (B) response to PB solution (base peak) and inhibition response to 44.2 ng mL^{-1} of Mb antigen. Reprinted from ref. [176] with permission of Elsevier.

ACCEPTED MANUSCRIPT

Figure 10. DPV signal responses of (A) AgNCs in situ-synthesized on the PDDA–Au/electrode; (B) PDDA–Au/HS-DNA/electrodes for (a) in the absence of target Thrombin, (b) in the presence of target Thrombin (1 nM) with DNAzyme amplification, (c) in the presence of target Thrombin (1 nM) with DNAzyme amplification and HCR (H_1 and H_2 without C-rich loop region), (d) in the presence of target Thrombin (1 nM) with DNAzyme and HCR double amplification (H_1 and H_2 with C-rich loop region)**.** Reprinted from ref. [12] with permission of Elsevier.

Figure 11. Binding interactions of CRP (contains two Ca^{2+} in each unit) within MIP cavities. Reprinted from ref. [183] with permission of Elsevier.

Figure 12. Analysis of each modification step. (A) Cyclic voltammograms for the modification processes. CV was carried out in PBS at scan rate of 100 mV/s. (B) Nyquist plots of the modification processes. Impedance was measured in PBS containing 5 mM $[Fe(CN)_6]^{3-/4-}$. Reprinted from ref. [189] with permission of Elsevier.

Figure 13. The fabrication of the anti-cTnI-Pt(MPA)-PMA/EG/GCE and) Nyquist plots of every step through fabrication of anti-cTnI-Pt(MPA)-PMA/EG/GCE in PBS (0.1 M KCl; pH 7.4) containing 2 mM $[Fe(CN)_6]^{3-/4-}$ **.** Reprinted from ref. [43] with permission of Elsevier.

ACCEPTED MANUSCRIPT

ACCEPTED MANUSCRIPT

Figures

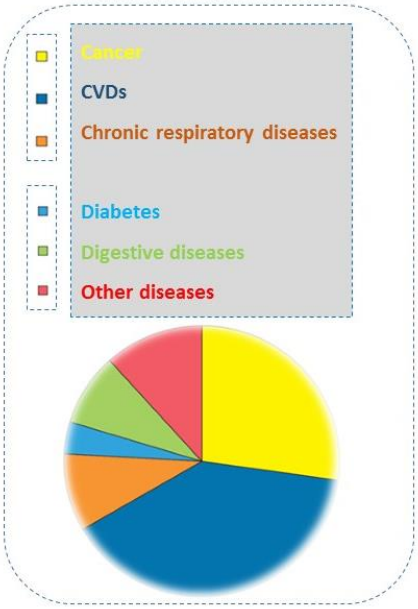

Figure 1. Global status report on leading causes of deaths in all over the world [1].

ACCEPTED MANUSCRIPT

ACCEPTED MANUSCRIPT

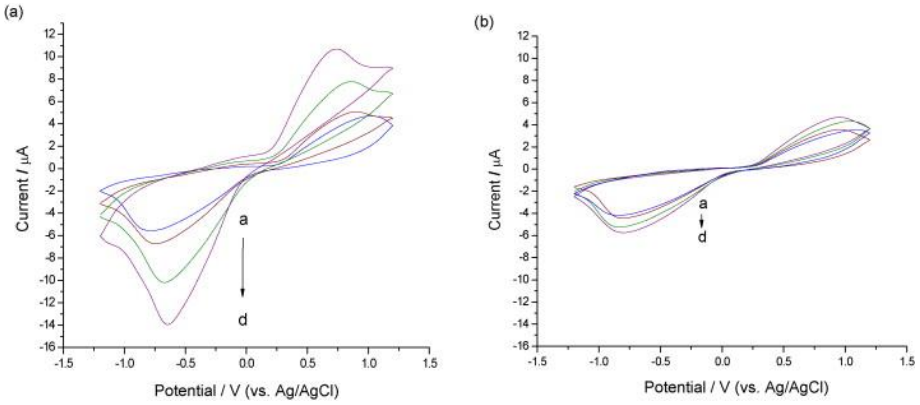

Figure 2. Cyclic voltammetry of SPEs at different concentrations of cTnT (1.0, 2.5, 5.0 and 10 ng mL^{-1}, (a)–(d), respectively), in the presence (a) and absence (b) of the microspheres on the epoxy-based composite. Reprinted from ref. [27] with permission of Elsevier.

ACCEPTED MANUSCRIPT

ACCEPTED MANUSCRIPT

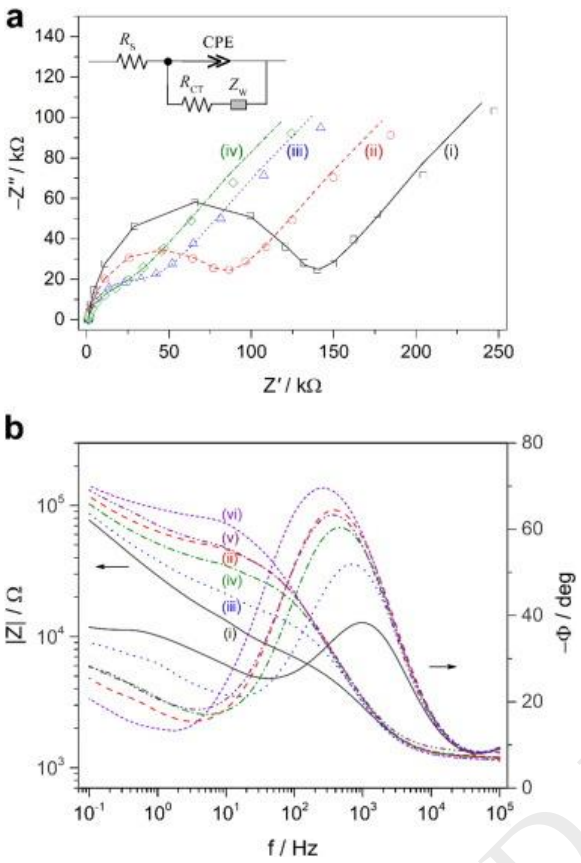

Figure 3. (a) Nyquist plots (Z' vs. $-Z''$) obtained from (i) ITO (□), (ii) NP/ITO (○), (iii) rGO/ITO (△) and (iv) rGO-NP/ITO (◇), each in 5 mM $[Fe(CN)_6]^{3-/4-}$ solution. The solid lines represents the experimental fit results to the measured data; (a, inset) Modified Randles equivalent circuit used to fit the experimental data to extrapolate impedance parameters; (b) Bode plots obtained after various steps of the process for (i,—) rGO-NP; (ii, – – –) MPA; (iii, ⋯) EDC-NHS; (iv, −·–) for anti-CRP; (v, −··–) for BSA and (vi, - - - -) for CRP (1 μg mL^{-1}) towards developing CRP detection sensor [6]. Reprinted from ref. [60] with permission of Elsevier.

ACCEPTED MANUSCRIPT

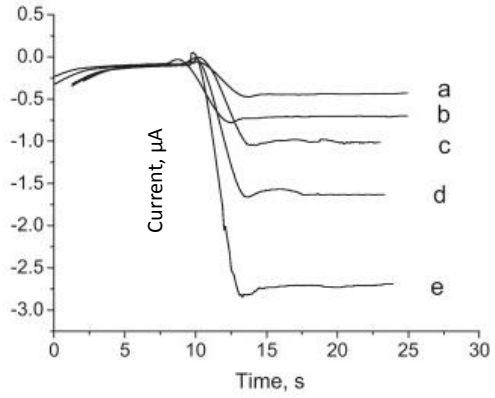

Figure 4. Electrochemical response of the PB-CeO_2 immunosensor at −0.2 V to 1 mM H_2O_2 after incubation with TNF-α of various concentrations. From a–e, 0.01, 0.05, 0.1, 0.5, 5 ng mL^{-1}. Reprinted from ref. [7] with permission of Elsevier.

ACCEPTED MANUSCRIPT

ACCEPTED MANUSCRIPT

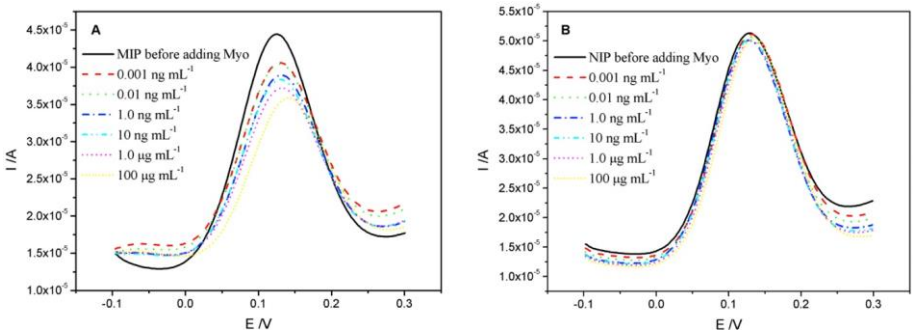

Figure 5. Electrochemical evaluation in presence of 5 mM $[Fe(CN)_6]^{3-/4-}$ redox probe of template rebinding with (A) MIP and (B) NIP receptor films, after incubation in different concentrations of MYO (from 0.001 ng mL^{-1} to 100 µg mL^{-1}, in 0.1 M PBS pH 7.0) for 10 min. Reprinted from ref. [8] with permission of Elsevier.

ACCEPTED MANUSCRIPT

ACCEPTED MANUSCRIPT

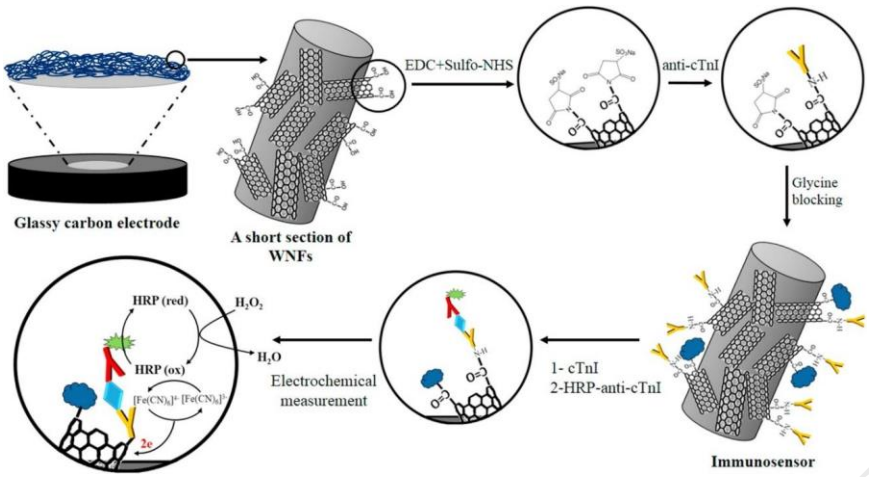

Figure 6. Schematic view of the stepwise fabrication of immunosensor and the mechanism of detection. Reprinted from ref. [171] with permission of Elsevier.

ACCEPTED MANUSCRIPT

ACCEPTED MANUSCRIPT

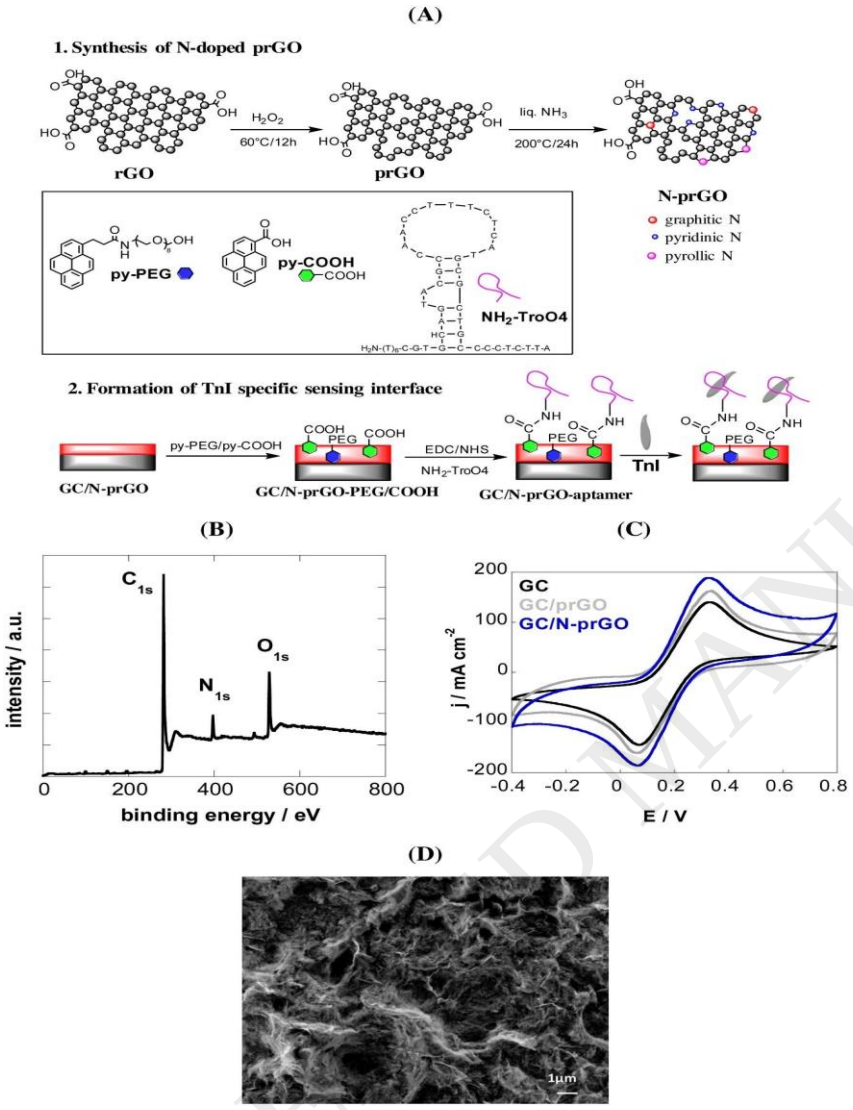

Figure 7. (A) The synthesis proces for N-prGO; (B) XPS results for N-prGO; (C) GC responses with cyclic voltammetry (black), GC/prGO (grey), and GC/N-prGO (blue) using $[Fe(CN)_6]^{4-}$ (5 mM)/PBS (0.1 M), scan rate = 100 mV s^{-1}; (D) morphology study of GC/N-prGO via SEM**.** Reprinted from ref. [172] with permission of Elsevier.

ACCEPTED MANUSCRIPT

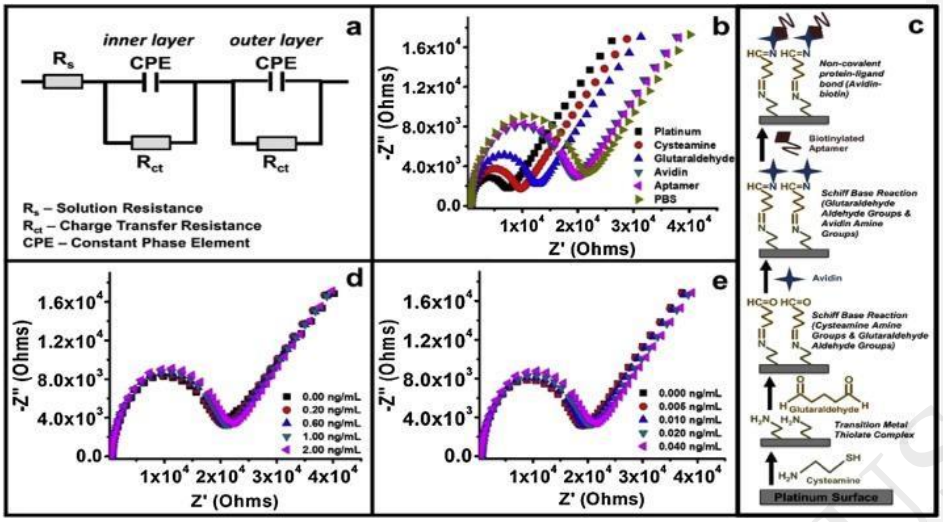

Figure 8. (a) Equivalent circuit, (b) Nyquist plots that conducted after each step of functionalization for the biosensor (10 mg mL^{-1} cysteamine, 25% glutaraldehyde, 1 mg mL^{-1} Neutravidin, and 150 µg mL^{-1} aptamer), (c) Functionalization process (d) Nyquist plots of EIS experiments conducted after each successive concentration of BNP demonstrating an increase in charge-transfer resistance with an increase in BNP concentration, (e) Nyquist plots of EIS experiments conducted after each successive concentration of TnT demonstrating an increase in charge-transfer resistance with an increase in TnT concentration. All EIS experiments were conducted in 5 mM ($Fe(CN_6)^{3-/4-}$) in 10 mM PBS, with 5 µm polished 0.5 mm diameter platinum working electrodes, Ag wire reference electrode, and Pt wire counter electrode across 300,000 Hz–0.01 Hz at 10 mV rms AC voltage. Reprinted from ref. [174] with permission of Elsevier.

ACCEPTED MANUSCRIPT

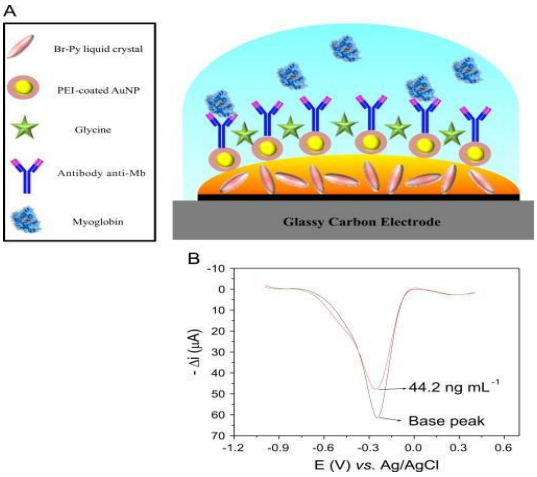

Figure 9. (A) Schematic representation of liquid crystal immunosensor surface, (B) response to PB solution (base peak) and inhibition response to 44.2 ng mL^{-1} of Mb antigen. Reprinted from ref. [176] with permission of Elsevier.

ACCEPTED MANUSCRIPT

ACCEPTED MANUSCRIPT

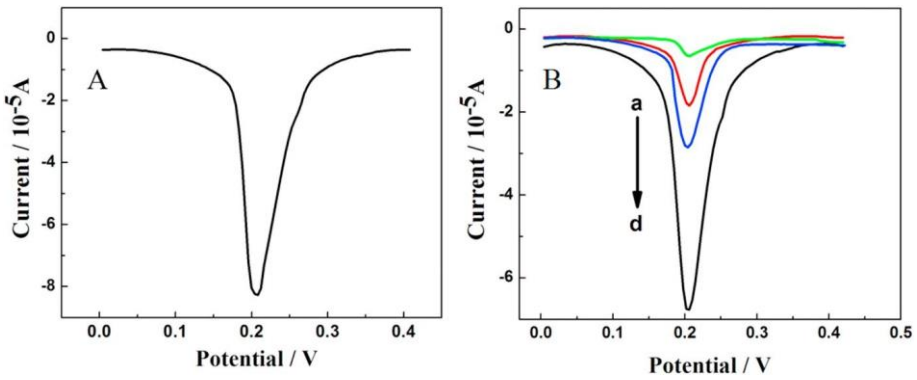

Figure 10. DPV signal responses of (A) AgNCs in situ-synthesized on the PDDA–Au/electrode; (B) PDDA–Au/HS-DNA/electrodes for (a) in the absence of target Thrombin, (b) in the presence of target Thrombin (1 nM) with DNAzyme amplification, (c) in the presence of target Thrombin (1 nM) with DNAzyme amplification and HCR (H_1 and H_2 without C-rich loop region), (d) in the presence of target Thrombin (1 nM) with DNAzyme and HCR double amplification (H_1 and H_2 with C-rich loop region)**.** Reprinted from ref. [12] with permission of Elsevier.

ACCEPTED MANUSCRIPT

ACCEPTED MANUSCRIPT

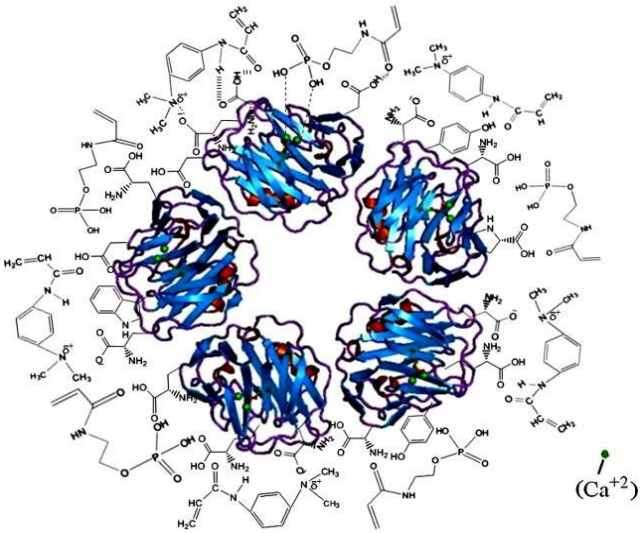

Figure 11. Binding interactions of CRP (contains two Ca^{2+} in each unit) within MIP cavities. Reprinted from ref. [183] with permission of Elsevier.

ACCEPTED MANUSCRIPT

ACCEPTED MANUSCRIPT

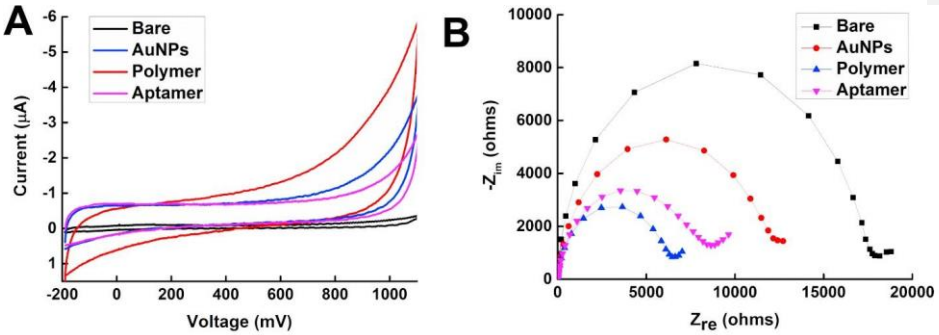

Figure 12. Analysis of each modification step. (A) Cyclic voltammograms for the modification processes. CV was carried out in PBS at scan rate of 100 mV/s. (B) Nyquist plots of the modification processes. Impedance was measured in PBS containing 5 mM $[Fe(CN)_6]^{3-/4-}$. Reprinted from ref. [189] with permission of Elsevier.

ACCEPTED MANUSCRIPT

ACCEPTED MANUSCRIPT

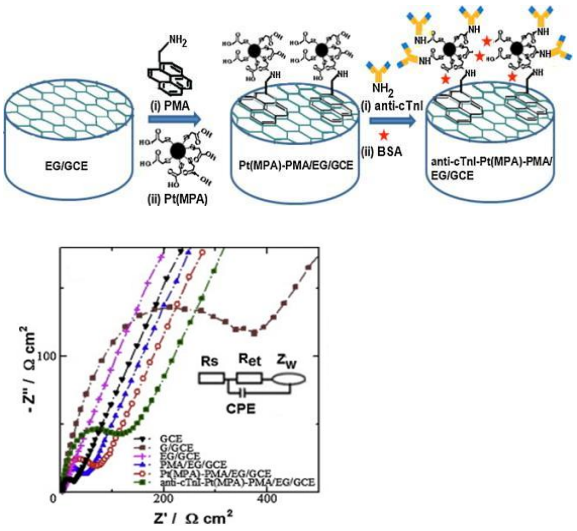

Figure 13. The fabrication of the anti-cTnI-Pt(MPA)-PMA/EG/GCE and) Nyquist plots of every step through fabrication of anti-cTnI-Pt(MPA)-PMA/EG/GCE in PBS (0.1 M KCl; pH 7.4) containing 2 mM $[Fe(CN)_6]^{3-/4-}$ **.** Reprinted from ref. [43] with permission of Elsevier.

ACCEPTED MANUSCRIPT

Table 1. Analytical parameters of clinical different biosensor platform recently used for Cardiac Troponin (cTnI&cTnT) biomarkers

Table 2. Analytical parameters of clinical different biosensor platform recently used for CRP biomarkers

Table 3. Analytical parameters of clinical different biosensor platform recently used for TNF-α biomarkers

Table 4. Analytical parameters of clinical different biosensor platform recently used for MYO biomarkers

Table 5. The cut-off level, accuracy, sensitivity and specificity values of cardiovascular biomarkers at admission and sixth hour time.

ACCEPTED MANUSCRIPT

ACCEPTED MANUSCRIPT

Table 1. Analytical parameters of clinical different biosensor platform recently used for Cardiac Troponin (cTnI&cTnT) biomarkers

Biomarker	Method	Transducer	Linearity Range	LOD/LOQ	Application	Reference
cTnI	EIS	Au/MHA/TMB/Den/anti-TnI/Au electrode	0.001 - 1.00 ng mL^{-1}	0.0002 ng mL^{-1}	Serum sample	[33]
cTnI	DPV	Anti-cTNI/ GQD / PAMAM/ Au electrode	-	20 fg mL^{-1}	Serum sample	[34]
cTnI	SWV	Ionic organic molecule/ CTS-AuNPs/GCE	0.20 - 1.00 ng mL^{-1}	0.10 ng mL^{-1}	Serum sample	[27]
cTnT	CV	Lateral flow membrane /SPE	0-700 ng mL^{-1}	0.15 ng mL^{-1}	-	[35]
cTnT	EIS	Anti-cTnT/COOH–CNT/PEI/Au electrode	0.1-10 ng mL^{-1}	0.033 ng mL^{-1}	Serum sample	[36]
cTnT	SWV	Fc/SiNps/ disk-type Au electrode	0.024−240 ng mL^{-1}	24 pg mL^{-1}	Serum sample	[37]
cTnI	CA	Sandwich aptamer/ SPCE	0.024–2.4 ng mL^{-1}	24 pg mL^{-1}	Serum sample	[38]
cTnT	DPV	MIP/ Au electrode	0.009–0.8 ng mL^{-1}	9 pg mL^{-1}	Serum sample	[39]
cTnT	DPV	AuNPs/Glycine/anti-cTnT/graphene/SPE	0.01-1.00 ng mL^{-1}	0.005 ng mL^{-1}	Serum sample	[29]
cTnI	DPV	GS/MWCNT/CS/GA/MIP/GCE	0.005 -60 ng mL^{-1}	0.0008 ng mL^{-1}	Serum sample	[40]
cTnI	CA	Poly(o-ABA)/GCE	0.05-5.0 ng mL^{-1}	0.016 ng mL^{-1}	Serum sample	[41]
cTnI	EIS	Anti-cTnI/ CNF nanoelectrode	0-10 ng mL^{-1}	0.2 ng mL^{-1}	-	[42]
cTnI	AdSSWV	Copper/C-dots@AuNP/ GA/CS/GCE	35 fg mL^{-1}- 350 ngmL^{-1}	11 fg mL^{-1}	Serum sample	[43]
cTnT	EIS	PAP/ FTO	-	18 ng mL^{-1}	-	
cTnI	AdSV	Anti-cTnI/ AuNP/ DDAB/SPE	0.1–32 ng mL^{-1}	0.1ng mL^{-1}	Serum sample	[45]
cTnT	CA	Streptavidin-microsphere/SPE	0.1- 10 ng mL^{-1}	0.2 ng mL^{-1}	Serum sample	[28]
cTnT	DPV	NH_2-CNT /SPE	0.0025-0.5 ng mL^{-1}	0.0035 ng mL^{-1}	Buffer solution	[46]
cTnT	DPV	MIP/graphene SPE	0.01- 0.1 ng mL^{-1}	0.006 ng mL^{-1}	Serum sample	[47]

ACCEPTED MANUSCRIPT

cTnT	EIS	anti-cTnI/PMA/EG/GCE	0.01–10 ng mL^{-1}	4.2 pg mL^{-1}	-	[48]
MYO cTnT	ASV	AgNps/SPE	-	200 pg mL^{-1} 150 pg mL^{-1}	-	[49]
cTnI	SWV	anti-cTnI/PdNP/SPE anti-cTnI /PtNP/SPE	0.1–40 ng mL^{-1} 0.1–55 ng mL^{-1}	0.1 ng mL^{-1} 0.07 ng mL^{-1}	-	[50]
cTnT	DPV	xGnP/AuNps-HEP/GCE	0.050-0.35 ng mL^{-1}	0.016 ng mL^{-1}	Serum sample	[51]
cTnI	EIS	Mn_3O_4-RGO/ microfluidic electrode	0.008−20 ng mL^{-1}	8.0 pg mL^{-1}	Serum sample	[52]
cTnl	CA	PDDA/RGO/Au electrode	0.1-10 ng mL^{-1}	0.024 ng mL^{-1}	Serum sample	[53]
cTnT	SWV	anti-cTnT/AuNps/ hybrid material/GCE	0.1-0.9 ng mL^{-1}	0.076 ng mL^{-1}	Serum sample	[54]
cTnI	EIS	Anti-cTnI/Ag(MPA)/ APTES/ITO	20 ng mL^{-1}-1 µg mL^{-1}	5.5 ng mL^{-1}	-	[55]
cTnI	CV	Anti-cTNI/AuNps/ITO	1-100 ng mL^{-1}	-	-	[30]

ACCEPTED MANUSCRIPT

Table 2. Analytical parameters of clinical different biosensor platform recently used for CRP biomarkers

Biomarker	Method	Transducer	Linearity Range	LOD/LOQ	Application	Reference
CRP	CA	CNTs/SPE	0.5 – 200 ng mL^{-1}	0.5 ng mL^{-1}	Serum sample	[67]
CRP	EIS	MUA /Au-SPE	-	-	-	[68]
CRP	EIS	GQD/GCE	10 -1466 ng mL^{-1}	3.68 ng mL^{-1}	Serum sample	[69]
CRP	EIS	HS-C_{11}-$(GR)_3$-OCH_2-COOH/Au electrode	10-1000 ng mL^{-1}	368 ng mL^{-1}	Serum sample	[70]
CRP	DPV	magnetic particles/ SPE	0 – 1000 mg L^{-1}	5.4x10^{-2} mg L^{-1}	Serum sample	[62]
NT-proBNP CRP	CA	MB/dual SPdCE	0 -4000 ng mL^{-1} 2.0 -100 ng mL^{-1}	0.47 ng mL^{-1}	Serum sample	[18]
CRP	CV	Au-SPE	0.52 -20 µg mL^{-1}	2.2 ng mL^{-1}	Serum sample	[71]
CRP	DPV	EDOTPC/GCE	209-3351 ng mL^{-1}	775 ng mL^{-1}	-	[72]
CRP	EIS	carbodiimide/anti-CRP/ VACNFs based NEAs	0- 87 ng mL^{-1}	11 ng mL^{-1}	-	[61]
CRP	EIS	anti-CRP/ protein G /Au	100-500 fg mL^{-1}	100 fg mL^{-1}	Serum sample	[73]
CRP	EIS	SAM/GA/CRP/CRP/Au electrode	1.15×10^{-5} - 1.15 mg L^{-1}	-	-	[74]
CRP	Potentiometry	monoclonal anti-CRP/GA/ZnO nanotubes	1.0×10^{-5} - 1.0 × 100 mg L^{-1}	-	Serum sample	[66]
CRP	EIS and CV	anti-CRP / thiol/carbodiimide/ Mo	100 pg mL^{-1}- 1 µg mL^{-1}	100 pg mL^{-1}	Synthetic urine sample	[75]
CRP	CA	Au microfluidic disc	0-25 ng mL^{-1}	4.9 pg mL^{-1}	Biological samples	[76]
CRP	DPV	anti-CRP/ STV-PbS QDs/graphite SPE	0.2-100 ng mL^{-1}	0.05 ng mL^{-1}	Serum sample	[63]
CRP	DPV	poly(3-ATP)/anti-CRP/ graphite	75 ng mL^{-1} - 150 µg mL^{-1}	7.24 µg mL^{-1}	Serum sample	[58]
CRP MPO	EIS	diatom membrane/ Au	1pg mL^{-1}-1µg mL^{-1}	1pg mL^{-1}	Serum sample	[77]
CRP	CA	Microfluidic disc	1-12.5 ng mL^{-1}	0.36 ng mL^{-1}	Serum sample	[78]
CRP-Ag	EIS	Anti-CRP/ZnS(MPA)-PPy /ITO	10 ng mL^{-1} -10 µg mL^{-1}	-	Buffer solution	[64]
CRP	EIS	Anti-αCRP/ Au(MPA)/ PPy/ITO	10 ng mL^{-1} -10 µg mL^{-1}	19.38 ng mL^{-1}	-	[79]
CRP	EIS	Pt(MPA)/ PPy bioelectrode	10 ng mL^{-1} - 10 µg mL^{-1}	4.54 ng mL^{-1}	Serum sample	[80]
CRP	EIS	anti-CRP/ protein G intermediate layer/Au	100 fg mL^{-1}- 1 ng mL^{-1}	100 fg mL^{-1}	Buffer solution	[25]
CRP	EIS	CRP- Ab(BSA)/ NHS/ MUA/ MPA/Au	45 ng mL^{-1}- 5.84 µg mL^{-1}	30 ng mL^{-1}	Buffer solution	[81]
CRP	EIS	Anti-CRP/PyNHS/rGO/SPCE	10 ng mL^{-1} -10 µg mL^{-1}	-	-	[82]

ACCEPTED MANUSCRIPT

CRP	DPV	anti-CRP/Au	6.25- 50 µg mL^{-1}	0.78 µg mL^{-1}	Serum samples	[83]
CRP	EIS	redox probe/Au	10.4–209.4 ng mL^{-1}	16.7 ng mL^{-1}	Phosphate buffer	[84]
CRP	EIS	Anti-CRP/Pt(MPA)–PMA/AG/GCE	10 ng mL^{-1} - 10 µg mL^{-1}	8.4 ng mL^{-1}	-	[61]
CRP	EIS	Anti-CRP/ssDNA/Au	3.125–25 mg L^{-1}	-	Serum samples	[85]
CRP	SWV	$Cu_3(PO_4)_2$/ PDA/rGO/GCE	0.5 pg mL^{-1} - 1 ng mL^{-1}	0.13 pg mL^{-1}	Serum sample	[86]
CRP	EIS	anti-CRP/ DSP/Au	1 pg mL^{-1} -1 µg mL^{-1}	-	Serum sample	[87]
CRP	EIS	anti-CRP/ NCD/Au	1.25 µg mL^{-1}	12.5 µg mL^{-1}	Serum sample	[88]
CRP	SWV	Zn^{2+}/Ab/Au NPs@SiMSs/GCE	0.005 -125 ng mL^{-1}	0.0017 ng mL^{-1}	Serum sample	[89]
CRP	EIS	rGO-NP/ITO	1 - 1000 ng mL^{-1}	0.06 ng mL^{-1}	Serum sample	[65]
CRP	EIS	GMI/Au	1-10 ng mL^{-1}	1 ng mL^{-1}	-	[90]
CRP sCD40L	DPV	rGO-TEPA/GCE	0.05 - 100 ng mL^{-1}	16.7pg mL^{-1} 13.1pg mL^{-1}	Serum sample	[91]
CRP	DPV	anti-CRP/AuNps/DNA/CuNps/GCE	1.0 fg mL^{-1}- 100 ng mL^{-1}	0.33 fg mL^{-1}	Serum sample	[92]
cTnI CRP	PEC	ALP/AChE/CdS/ TiO_2 NTs electrode	50 ng mL^{-1} -50 µg mL^{-1} 0.1 ng mL^{-1}- 5 µg mL^{-1}	-	-	[93]
CRP	DPV	MoS_2–PANI–GNPs/GCE	0.2 - 80 ng mL^{-1}	40 pg mL^{-1}	Serum sample	[94]
cTnI CRP	AdSSWV	anti-cTnI, anti-CRP/PDMS-GNP/Microfluids disc	0.01-50 µg L^{-1} 0.5-200 µg L^{-1}	5 amol/30 µL 307 amol/30 µL	Serum sample	[95]

ACCEPTED MANUSCRIPT

Table 3. Analytical parameters of clinical different biosensor platform recently used for TNF-α biomarkers

Biomarker	Method	Transducer	Linear Range	LOD/LOQ	Application	Reference
TNF-α	DPV	anti-TNF-α/ AuNps/ MWCNTs/ ionic liquid/GCE	6.0-100 pg mL^{-1}	2.0 pg mL^{-1}	Serum sample	[105]
TNF-α	DPV	AuNps/DOXh/Au	1-1000 pg mL^{-1}	0.7 pg mL^{-1}	Serum sample	[106]
TNF-α	CA	GR/PtNps3 matrix/ protoporphyrin IX/ graphene paste electrode	1-100 pg mL^{-1}	1pg mL^{-1}	Children's cerebrospinal fluid sample	[107]
TNF-α	DPV	Apt-Ag@Pt-GRs/SPE	5.0 - 70 pg mL^{-1}	1.64 pg mL^{-1}	Serum sample	[108]
TNF-α	DPV	Ag@Pt-CNTs–CS/SPE	6.0-60 pg mL^{-1}	1.6 pg mL^{-1}	Serum sample	[109]
TNF-α	CA	protoporphyrin/diamond paste electrode	-	10 pg mL^{-1}	Cerebrospinal fluid sample	[110]
TNF-α	SWV	anti-TNF-α /Fc-PNW/GNR PDDA/GCE	0.005–10 ng mL^{-1}	2 pg mL^{-1}	Serum sample	[111]
TNF-α	DPV	AuNps/ poly (styrene-acrylic acid)/ALP-Ab2-GNPs/PSA/GCE	0.02–200 ng mL^{-1}	0.01 ng mL^{-1}	Serum sample	[112]
TNF-α	CA	PB-CeO2/CS/ Ab1/AuNps/CNT/GCE	0.005–5 ng mL^{-1}	2 pg mL^{-1}	Serum sample	[104]
TNF- α	CV	anti-TNF- α/K-CS-GA/GCE	0.02–34 ng mL^{-1}	10 pg mL^{-1}	Serum sample	[113]
TNF- α	DPV	CB/AuNps/CS	0.001-100 ng mL^{-1}	0.5 pg mL^{-1}	Serum sample	[114]
TNF- α	SWV	Fc/ Phe/GCE	1 pg mL^{-1}-10 ng mL^{-1}	0.5 pg mL^{-1}	Serum sample	[115]
TNF- α	EIS	anti- TNF- α/DSP/Au	1–100 pg mL^{-1}	~1.4 pg mL^{-1}	Cell culture	[116]
TNF- α	DPV	Ag@Pt-GRs/Au SPE	0-60 pg mL^{-1}	2.07 pg mL^{-1}	Serum sample	[117]
TNF- α	EIS	anti-TNF-α/Au	1- 15 pg mL^{-1}	-	Artificial human saliva	[118]
TNF- α	SWV	10 mM aptamer/Au	10 - 100 ng mL^{-1}	10 ng mL^{-1}	Serum sample	[119]
TNF- α	DPV	Affibodys/MYO/SPE	76–5000 pg mL^{-1}	38 pg mL^{-1}	Serum sample	[120]
TNF- α	DPV	SB/EA/anti-TNF-α/DSP/Au	500 pg mL^{-1} - 100ng mL^{-1}	60 pg mL^{-1}	Serum sample	[100]
TNF- α	DPV	MMeELISA	0.48-2000pg mL^{-1}	0.48 pg mL^{-1}	Gingival crevicular fluid sample	[121]
TNF- α	DPV	anti-TNF-α/C60–CNTs–IL/SPE	5.0 -75 pg mL^{-1}	2.0 pg mL^{-1}	Serum sample	[101]
TNF- α	DPV	Anti-TNF-α/FNAB/PC/ Au	100pg mL^{-1}-100 ng mL^{-1}	100 pg mL^{-1}	Serum sample	[122]

ACCEPTED MANUSCRIPT

TNF- α	EIS	MYO/Anti- TNF- α/ Au	1–1000 pg mL^{-1}	1 pg mL^{-1}	Serum sample	[102]
IL-6, IFN-γ, TNF -α IL-8	DPV	MEEPS	10 ng mL^{-1}–20 μg mL^{-1}	10 ng mL^{-1}	-	[123]
TNF -α	EIS	anti-TNF-α/CMA/Au	266 pg mL^{-1}- 666 ng mL^{-1}	-	-	[94]
TNF -α	EIS	anti-TNF-α/P3/ITO	0.01-2 pg mL^{-1}	3.7 fg mL^{-1}	Human serum and saliva sample	[124]
TNF –α IL-1β	CA	HOOC-Phe-DWCNTs/SPCEs	1- 200 pg mL^{-1} 0.5-100 pg mL^{-1}	0.85 pg mL^{-1} 0.38 pg mL^{-1}	Human serum spiked Real saliva sample	[103]
TNF -α	EIS	anti-TNF- α/carboxyl diazonium/Au	1-15 pg mL^{-1}	3.1 pg mL^{-1}	Real human saliva	[125]
TNF -α	SWV	MB/thiolated Au	9-88ng mL^{-1}	5.46 ng mL^{-1}	Cell culture	[126]
TNF -α	SWV	MBs/SPCEs	2.0-5.8 pg mL^{-1}	2.0 pg mL^{-1}	Serum sample	[127]

Table 4. Analytical parameters of clinical different biosensor platform recently used for MYO biomarkers

Biomarker	**Method**	**Transducer**	**Linear Range**	**LOD/LOQ**	**Application**	**Reference**
MYO	EIS	Anti-MYO /4-ATP SAM/Au	350 ng mL^{-1} -17.5 μg mL^{-1}	5.5 ng mL^{-1}	Saline and serum samples	[132]
MYO	EIS	Ab-MYO/AuNps/APTES /ITO	10 ng mL^{-1}-1 μg mL^{-1}	2.7 ng mL^{-1}	Serum sample	[136]
MYO	CA	PAP/PQI/IDAcarbon nanoelectrode	0.001–100 ng mL^{-1}	0.4 pg mL^{-1}	Saline and human serum sample	[137]
MYO	EIS	Anti-MYO-IgG/MWCNT/SPE	0.1–90 ng mL^{-1}	0.08ng mL^{-1}	Serum sample	[138]
MYO	CV	CuS–MoS_2/Anti-MYO/FME	0.005–20 ng mL^{-1}	1.2 pg mL^{-1}	Serum sample	[139]
MYO	DPV	MBA/AuNps/RGD/GR-COOH/GCE	0.0001-0.2 g L^{-1}	26.3 ng mL^{-1}	Pork samples	[140]
MYO	DPV	TCPP–Gr/AuNps/GCE	0.35 ng mL^{-1}-13.4 μg mL^{-1}	0.11 ng mL^{-1}	Serum sample	[141]
MYO	EIS	Anti-MYO/PtNP(PPy-PPa)-RGO/ITO	10 ng mL^{-1}-1 μg mL^{-1}	4.0ng mL^{-1}	-	[142]

ACCEPTED MANUSCRIPT

MYO	DPV	DSP/SAM/Au	17.8-1780 ng mL^{-1}	9.8 ng mL^{-1}	Serum sample	[143]
MYO	DPV	MIP/MWCNT/GCE	1 µg mL^{-1}- 0.1 mg mL^{-1}	0.17 µg mL^{-1}	Serum sample	[144]
MYO	DPV	DApt/ Exo I/ Au	0- 1.4 µg mL^{-1}	0.47 ng mL^{-1}	Serum sample	[145]
MYO	SWV	MIP/AuSPE	0.001 ng mL^{-1} -100 µg mL^{-1}	14 pg mL^{-1}	Serum sample	[133]
MYO	SWV	MIP/PVC-COOH/ Au-SPE	1.1-2.98 µg mL^{-1}	2.25 µg mL^{-1}	Serum sample	[146]
MYO	SWV	SPAM/Au-SPE	0.59-18.77 µg mL^{-1}	0.28 µg mL^{-1}	Spiked biological fluid sample	[147]
MYO	SWV EIS	PAP/Au-SPE	3.53 - 53.3 µg mL^{-1}	2.22 µg mL^{-1}	Serum sample	[148]
MYO	EIS	Anti-MYO/GQDs/ SPE	0.01–100 ng mL^{-1}	0.01 ng mL^{-1}	Serum sample	[149]
MYO	DPV	MWCNT/MIP/SPE	-	-	Serum sample	[150]
MYO	SWV	Ab-MYO/AuNp DDAB/SPE	-	-	-	[151]
MYO	EIS	Ab-MYO(BSA)/ ZnS(MPA)–RGO/APTES/ITO	10 ng mL^{-1} -1 µg mL^{-1}	-	-	[152]
IgG MYO	CA	PANI nanowire/ Anti-MYO/Au	5 ng mL^{-1} -2.5 µg mL^{-1} 5 ng mL^{-1}- 2.78 µg mL^{-1}	3 ng mL^{-1} 1.4 ng mL^{-1}	-	[153]
MYO	CV	Ti-NT/GCE	0.001- 0.1 mg mL^{-1}	1 µg mL^{-1}	Serum sample	[130]
MYO	CV	PLL/BP/anti-MYO DNA aptamers/SPE	1 pg mL^{-1} -16 µg mL^{-1}	0.524 pg mL^{-1}	Serum sample	[154]
MYO	EIS	Pt(MPA)/Anti-MYO/ ITO	0.01 µg mL^{-1} - 1 µg mL^{-1}	sub-µg mL^{-1}	Serum sample	[155]
MYO	EIS	PPy-PPa/RGO/ ITO	10 ng mL^{-1}- 1 µg mL^{-1}	-	Serum sample	[128]
MYO	CV	rGO/CNT/SPE	1 ng mL^{-1} - 4 mg mL^{-1}	0.34 ng mL^{-1}	-	[156]
MYO	DPV	AuNp@rGO/SPE	1ng mL^{-1} -1400 ng mL^{-1}	0.67 ng mL^{-1}	Serum sample	[157]
MYO	EIS	Anti-MYO(BSA)/ ZnS(MPA)/APTES/ITO	10 ng mL^{-1}- 1 µg mL^{-1}	-	-	[158]
MYO	SWV	AuNp/DDAB/Anti-MYO/SPE	10–1780 ng mL^{-1}	10ng mL^{-1}	Serum sample	[159]
CK-MYO	SWV	Pcrea/Au-SPE	0.48-28.8 µg mL^{-1}	0.11 µg mL^{-1}	Serum sample	[160]
MYO	CV	Nafion/MYO/Au/GR/CILE	34.6 µg mL^{-1}-	11.5 µg mL^{-1}	-	[161]

ACCEPTED MANUSCRIPT

			238.2 mg mL^{-1}			
MYO	CV	CS/MYO-Fe_3O_4@SiO_2/CILE	0.2 -11.0 ng mL^{-1}	0.18 ng mL^{-1}	-	[162]
MYO	ASV	AgNps/SPCE	-	3 ng mL^{-1}	-	[131]
CK	EIS	Ab-CK/Au(MPA)/ APTES/ITO	10 ng mL^{-1}- 0.5 µg mL^{-1}	5.3 ng mL^{-1}	Serum sample	[163]
MYO	EIS	AuNp-PPy-PPa/RGO/APTES/ITO	10 ng mL^{-1}-1 µg mL^{-1}	1.49 ng mL^{-1}	Serum sample	[164]

ACCEPTED MANUSCRIPT

Table 5. The cut-off level, accuracy, sensitivity and specificity values of cardiovascular biomarkers at admission and sixth hour time.

	Cut-off level	***Predictive accuracy***	***Common sensitivity and specificity***
At admission time			
cTnT (ng mL^{-1})	0.05	0.643	52%
MYO (ng mL^{-1})	23	0.623	63%
CRP (mg dL^{-1})	0.31	0.662	66%
CK-MB (ng dL^{-1})	2.0	0.721	72%
Serum fibrinogen (mg dL^{-1})	360	0.701	69%
cTnI (ng mL^{-1})	0.30	0.870	86%
At 6 h control			
cTnT (ng mL^{-1})	0.05	0.612	61%
MYO (ng mL^{-1})	26.0	0.617	63%
CK-MB (ng mL^{-1})	2.5	0.734	73%
CRP (mg dL^{-1})	0.55	0.682	72%
cTnI (ng mL^{-1})	0.5	0.909	83%

ACCEPTED MANUSCRIPT